

Natural anomaly-mediation from the landscape with implications for LHC SUSY searches

Howard Baer^{1*}, Vernon Barger^{2†}, Jessica Bolich^{1‡}
Juhi Dutta^{1§} and Dibyashree Sengupta^{3¶}

¹*Department of Physics and Astronomy, University of Oklahoma, Norman, OK 73019, USA*

²*Department of Physics, University of Wisconsin, Madison, WI 53706, USA*

³*INFN, Laboratori Nazionali di Frascati, Via E. Fermi 54, 00044 Frascati (RM), Italy*

Abstract

Supersymmetric models with the anomaly-mediated SUSY breaking (AMSB) form for soft SUSY breaking terms arose in two different settings: **1**) extra-dimensional models where SUSY breaking occurred in a sequestered sector and **2**) $4 - d$ models with dynamical SUSY breaking in a hidden sector where scalars gain masses of order the gravitino mass $m_{3/2}$ but gaugino masses and trilinear soft terms assumed to be of the AMSB form. Both models have run into serious conflicts with 1. LHC sparticle and Higgs mass constraints, 2. constraints from wino-like WIMP dark matter searches and 3. bounds from naturalness. These conflicts may be avoided by introducing minor changes to the underlying phenomenological models consisting of non-universal bulk scalar Higgs masses and A -terms, providing a setting for *natural anomaly-mediation* (nAMSB). In nAMSB, the wino is still expected to be the lightest of the gauginos, but the higgsinos are expected to be the lightest electroweakinos (EWinos) in accord with naturalness. We examine what sort of spectra are expected to emerge when nAMSB arises from a string landscape setting: while model **2** can only be natural for a Higgs mass $m_h \lesssim 123$ GeV, model **1** can accommodate naturalness along with $m_h \sim 125$ GeV whilst still respecting LHC bounds on sparticle masses. We explore the LHC phenomenology of nAMSB models where we find that for higgsino pair production, typically larger dilepton mass gaps arise from the soft dilepton-plus-jets signature than in models with gaugino mass unification. For wino pair production, the higher $m_{3/2}$ portion of nAMSB parameter space is excluded by recent LHC bounds from gaugino pair production searches. We characterize the dominant LHC signatures arising from the remaining lower $m_{3/2} \sim 90 - 200$ TeV range of parameter space which should be fully testable at high-luminosity LHC via EWino pair production searches.

*Email: baer@nhn.ou.edu

†Email: barger@pheno.wisc.edu

‡Email: Jessica.R.Bolich-1@ou.edu

§Email: juhi.dutta@ou.edu

¶Email: Dibyashree.Sengupta@lnf.infn.it

1 Introduction

Supersymmetric models[1] based on anomaly-mediated SUSY breaking (AMSB) arose from two different set-ups.

1.1 AMSB0: (GLMR)

The second, by Giudice *et al.*[2] (GLMR), which we label as *AMSB0*, was motivated by 4-dimensional models where SUSY is broken dynamically in the hidden sector[3], and where SUSY breaking was communicated to the visible sector via gravity. The motivation here was that the SUSY breaking scale m_{hidden} might be generated non-perturbatively via gaugino condensation and would then be exponentially-suppressed relative to the Planck scale via dimensional transmutation[4]: $m_{hidden} \sim e^{-8\pi^2/g^2} m_P$, where m_P is the reduced Planck scale. This would not only stabilize the weak scale (via SUSY), but also explain its exponential suppression from the Planck scale: $m_{weak} \sim m_{soft} \sim m_{hidden}^2/m_P$, where $m_{hidden} \sim 10^{11}$ GeV. Now in gravity mediation, gaugino masses arise via

$$\int d^2\theta f_{AB} \left(\frac{S}{m_P} \right) W_\alpha^A W^{B\alpha} \quad (1)$$

with f_{AB} the gauge kinetic function depending on hidden sector fields S and where the F -term of S acquires a SUSY breaking value F_S ; the gaugino masses arise as $m_\lambda \sim (F_S/m_P) \sim m_{3/2} \sim m_{soft} \sim m_{weak}$. However, if no hidden sector singlets are available as in (most) DSB models[5]¹, then the gaugino masses are expected instead at the keV scale, which would be experimentally excluded. However, Ref. [2] found that the one-loop renormalization of the visible sector gauge couplings is given by[7]

$$\frac{1}{4} \int d^2\theta \left(1 - \frac{g^2 b_0}{16\pi^2} \log \frac{\Lambda^2}{\square} \right) W^\alpha W_\alpha + h.c. \quad (2)$$

where b_0 is the coefficient of the relevant gauge group beta-function and \square is the d'Alembertian operator. This leads to SUSY breaking gaugino masses via replacement of the UV cutoff Λ by the spurion superfield $\Lambda \exp(m_{3/2}\theta^2)$ leading to (loop-suppressed) gaugino masses[8]²

$$m_\lambda = -\frac{g^2 b_0}{16\pi^2} m_{3/2}. \quad (3)$$

For $m_{3/2} \sim 100$ TeV, then $m_\lambda \sim 1$ TeV as required to gain $m_{weak} \sim m_{W,Z,h} \sim 100$ GeV. Similarly, the trilinear soft (A)-terms are not allowed at tree level if no singlets are available for a

$$\int d^2\theta \frac{S}{m_P} \phi_i \phi_j \phi_k \quad (4)$$

coupling (where the ϕ_i are generic visible sector superfields). The A -terms can also arise at one-loop level in AMSB and are proportional to derivatives of the anomalous dimensions. Scalar

¹For an exception, see *e.g.* [6].

²The AMSB contributions to gaugino masses were already presaged by Ref's [9], [10] and [11, 12].

masses on the other hand arise from

$$\int d^2\theta d^2\bar{\theta} \frac{S^\dagger S}{m_P^2} \phi^\dagger \phi \quad (5)$$

and are not protected by symmetries and so can be much larger, $m_\phi^2 \sim m_{3/2}^2$, and can gain their gravity-mediated form. This form of scalar mass generation suffers the usual SUSY flavor problem that is endemic to gravity-mediation.

The AMSB0 model thus yields a hierarchy of soft terms $m_\phi \gg m_\lambda \sim A$ as noted by Wells[13] in what he dubbed PeV-SUSY[14]. This model also motivated realizations of split[15, 16]- and minisplit[17] SUSY models. These later models eschew the notion of naturalness in hopes of a landscape solution to the naturalness problem, thus allowing for scalar masses in the range of 100-1000 TeV (for minisplit) and ranging up to $m_\phi \sim 10^9$ TeV for split SUSY. Split SUSY predicts a light Higgs mass $m_h \sim 130 - 160$ GeV[18]. The discovery of a SM-like Higgs boson with mass $m_h \sim 125$ GeV motivated a retreat to scalars in the range of minisplit models which allow for $m_h \sim 125$ GeV along with small A -terms. A value of $m_h \simeq 125$ GeV can also be realized by TeV-scale top squarks but with near maximal stop mixing from large A -terms[19, 20].

Since scalar masses arise as in gravity-mediation, this *AMSB0* model may still be plagued by flavor problems, although these may be softened by the rather large values of scalar masses which are expected: a (partial) decoupling solution to the SUSY flavor problem[21]. It also gave rise to unique phenomenological signatures[22] since in AMSB the *wino* rather than the bino was expected to be the lightest SUSY particle (LSP).

1.2 AMSB (RS)

Alternatively, in the Randall-Sundrum AMSB model[23] (*AMSB*), it was posited that SUSY breaking arose in a hidden sector sequestered from the visible sector in extra-dimensional space-time. In such a set-up, the leading contribution to *all* soft SUSY breaking terms was from the superconformal anomaly, and suppressed by a loop factor from the gravitino mass $m_{3/2}$. In this form of AMSB, a common value of scalar masses was expected thus avoiding the SUSY flavor problem which seems endemic to models of gravity-mediation. Also, since $m_{soft} \ll m_{3/2}$, the cosmological gravitino problem could be avoided since in the early universe thermally-produced gravitinos could decay before the onset of BBN[24]. In both cases of *AMSB* and *AMSB0*, the thermally underproduced wino-like WIMPs could have their relic abundance non-thermally enhanced by either gravitino[25] or moduli-field decays[26, 27]. A drawback in the case of *AMSB* was that soft slepton masses were derived to be *tachyonic* thus leading to charge-breaking vacua in the scalar potential. Some extra contributions to scalar masses arising from fields propagating in the bulk of spacetime could be postulated to avoid this problem[23].

1.3 Further deliberations on AMSB

Some further notable theoretical explorations of AMSB soft terms include Gaillard *et al.*[28] where AMSB soft terms arose as quantum corrections under Pauli-Villars regularization of supergravity. In Anisimov *et al.*[29, 30], brane world SUSY breaking (as in RS model) was examined, and it was found to be insufficient to guarantee the needed sequestering between

hidden and observable sectors to generate dominant AMSB soft terms and flavor-conserving scalar masses. In Ref. [31], Luty presents pedagogical lectures on SUSY breaking leading up to and including AMSB. In Ref. [32], the connection of AMSB to dimensional transmutation is examined as a solution to the tachyonic slepton problem. In Ref. [33], Dine and Seiberg (DS) clarify the derivation of AMSB soft terms and relate them to the gaugino counterterm. In Ref. [34], de Alwis presents the derivation of AMSB soft terms and emphasizes their origin in work by Kaplunovsky and Louis[12] and DS, and shows there may be additional soft term contributions. This inspires his later development of the gaugino AMSB model[35]. In Ref. [36], a clarifying derivation of AMSB soft terms is presented. In Ref. [37], Sanford and Shirman develop an arbitrary conformal compensator formalism which allows extrapolation between RS and DS derivations. In Ref. [38], anomaly mediation from IIB string theories is examined. In Ref. [39], the AMSB connection to gravitino mediation vs. Kähler mediation is examined. This work is extended to scalar masses in Ref. [40]. In Ref. [41], Dine and Draper examine anomaly mediation in local effective theories. In Ref. [42], de Alwis examines the interplay of AMSB with spontaneous SUSY breaking. In Ref. [43], the connection between AMSB gaugino masses and the path integral measure is examined.

An alternative route to models with AMSB soft terms was developed by Luty and Sundrum[44], in models with strong hidden sector conformal dynamics. In these $4 - d$ models, strong hidden sector conformal dynamics leads to a suppression, or sequestering, of usual soft terms due to higher dimensional operators which mix the hidden and visible sectors. The suppression of gravity-mediated soft terms occurs between the messenger scale (taken here to be m_P) and some intermediate scale m_{int} where conformal symmetry becomes broken. In such a case, the loop-suppressed AMSB soft terms may become dominant. In Ref. [45], the conformal suppression acts upon scalar masses and the $B\mu$ term, but in Ref's [46, 47] it is emphasized that conformal sequestering may also act on the gaugino sector.

1.4 Status of minimal phenomenological AMSB model (mAMSB)

A minimal phenomenological AMSB model (mAMSB) was proposed in Ref's [48] and [49] with parameter space

$$m_0, m_{3/2}, \tan \beta, \text{sign}(\mu) \quad (mAMSB) \quad (6)$$

where m_0 was an added universal bulk scalar mass and the gravitino mass $m_{3/2}$ set the scale for the AMSB soft terms $m_{AMSB} \sim c(g^2/16\pi^2)m_{3/2}$ with c a calculable constant of order unity and g is a gauge group coupling constant. The bulk scalar mass is generic to the *AMSB0* set-up and phenomenologically required to gain positive slepton squared masses in *AMSB*. Various studies for mAMSB at LHC appeared in Ref's [50, 51, 52, 53, 54].

At present, both these set-ups within the mAMSB model seem phenomenologically disfavored and perhaps even ruled out. The first problem is that in mAMSB the SUSY conserving μ parameter is typically fine-tuned to large values compared to the measured value of the weak scale $m_{weak} \sim m_{W,Z,h} \sim 100$ GeV, thus violating[55] even the most conservative measure of naturalness Δ_{EW} [56, 57], where Δ_{EW} is defined as the largest value on the right-hand-side

(RHS) of the scalar potential minimization condition

$$m_Z^2/2 = \frac{m_{H_d}^2 + \Sigma_d^d - (m_{H_u}^2 + \Sigma_u^u) \tan^2 \beta}{\tan^2 \beta - 1} - \mu^2 \quad (7)$$

divided by $m_Z^2/2$. The second problem is that the small values of mAMSB A -terms typically lead to too small a value of $m_h \ll 125$ GeV unless third-generation soft scalar masses lie in the 10-100 TeV range[58, 59] thus also violating naturalness[55] via the radiative corrections $\Sigma_u^u(\tilde{t}_{1,2})$, leading again to a large value for the electroweak fine-tuning measure Δ_{EW} . A third problem is that wino-only dark matter[26] now seems excluded by a combination of direct and indirect WIMP search experiments[60, 61, 62]. This latter exclusion may be circumvented in cases of mixed axion-wino dark matter (two DM particles) wherein the relic wino abundance forms only a small portion of the total DM abundance[63]. This latter scenario posits a PQ axion which also solves the finetuning problem of the θ parameter in the QCD sector.

1.5 Natural anomaly-mediated SUSY breaking (nAMSB)

In Ref. [64], two minor changes to the mAMSB model were suggested to circumvent its undesirable phenomenological properties.³ First, separate bulk masses for $m_{H_u} \neq m_{H_d} \neq m_0$ were applied to scalar masses which then allowed for a small μ parameter in accord with naturalness (a unified mass m_0 just for matter scalars is highly motivated by the fact that the matter superfields are unified within the 16-dimensional spinor rep of $SO(10)$). Second, bulk contributions to trilinear soft terms A_0 were advocated which then allowed for large stop mixing which in turn uplifts the Higgs mass $m_h \rightarrow \sim 125$ GeV[65] without requiring the stop sector to lie in the unnatural multi-TeV range or beyond. These two adjustments allowed for EW naturalness and for $m_h \sim 125$ GeV. Models with these attributes were denoted as *natural* AMSB (nAMSB):

$$m_0(i), m_{H_u}, m_{H_d}, m_{3/2}, A_0, \tan \beta \quad (nAMSB') \quad (8)$$

where we also allow for possible non-universal bulk contributions to the different generations $i = 1 - 3$. It is convenient to then trade the high scale parameters $m_{H_u}^2$ and $m_{H_d}^2$ for weak scale parameters μ and m_A using the scalar potential minimization conditions[66, 67].

Like mAMSB, the nAMSB model has winos as the lightest of the gauginos. Unlike mAMSB, the nAMSB model (usually) has *higgsinos as the lightest EWinos*, in accord with naturalness. By requiring the natural axionic solution to the strong CP problem, one then expects mixed axion plus higgsino-like WIMP dark matter[68, 69], and one can circumvent the constraints on wino-only dark matter[62].

1.6 nAMSB from the landscape

The advent of the string theory landscape[70, 71] led to some major changes in SUSY models with AMSB soft terms. First, it was found that flux compactification[72] of type IIB string models on Calabi-Yao orientifolds led to enormous numbers of string vacuum states (10^{500} is a prominently quoted number[73, 74] although much larger numbers have also been

³These “changes” were actually suggested as default parameters in the original RS paper Ref. [23].

found in F -theory compactifications[75]). Such large numbers of vacuum possibilities allow for Weinberg’s[76] anthropic solution to the cosmological constant (CC) problem and “explains” the finetuning of Λ_{CC} to a part in 10^{120} . Then, if the CC is finetuned by anthropics, might one also allow for the little hierarchy $m_{weak} \ll m_{soft}$ to also be finetuned? In split SUSY, electroweak naturalness is eschewed while WIMP dark matter and gauge coupling unification are retained[13, 15, 77]. A possible model framework for split SUSY would then be charged SUSY breaking[16, 14], wherein tree level gaugino masses (and A -terms) are forbidden by some symmetry (perhaps R -symmetry?) while scalar masses are allowed as heavy as one likes. Values of $m_{scalar} \sim 10^9$ GeV were entertained, leading to a signature of long-lived gluinos. The heavy scalars also allowed for a decoupling solution to the SUSY flavor and CP problems[21]. In split SUSY, one expects light Higgs masses in the $m_h \sim 130 - 160$ GeV range[18, 78], in contrast to the 2012 Higgs discovery with $m_h \simeq 125$ GeV. To accommodate the measured Higgs mass, scalar masses were dialed down to the 10^3 TeV range. These *minisplit* models[17, 79] then allowed for $m_h \sim 125$ GeV while still potentially allowing for a decoupling solution to the SUSY flavor and CP problems.

However, only recently has the occurrence frequency of highly finetuned SUSY models been examined in an actual landscape context. In Ref. [80], a toy model of the landscape was developed, and it was shown that EW *natural* models should be more likely than finetuned models to emerge from a generic landscape construction. In retrospect, the reason is rather simple. In Agrawal *et al.*[81] (ABDS), it was found that within a multiverse wherein each pocket universe would have a different value for its weak scale, then only complex nuclei, and hence complex atoms (which seem necessary for life as we know it) would arise if the pocket universe value of the weak scale were within a factor of a few of its measured value in our universe (OU): $0.5m_{weak}^{OU} \lesssim m_{weak}^{PU} \lesssim 5m_{weak}^{OU}$. We call this range of m_{weak}^{PU} the ABDS window. Now in models where all contributions to the weak scale (to the RHS of Eq. 7) are natural (in that they lie within the ABDS window), then the remaining parameter selection (typically either $\mu(weak)$ or $m_{H_u}(weak)$) will also have a wide range of possibilities, all lying within the ABDS window, to gain an ultimate value for m_{weak} within the ABDS window. On the other hand, if any contribution to m_{weak} is far beyond m_{weak} , then finetuning is needed and only a tiny portion of parameter space will lead to $m_{weak} \sim 100$ GeV. This scheme was then used in Ref. [82] to compute relative probabilities P_μ for different natural and finetuned SUSY models (and the SM) to emerge from the landscape. For instance, from Ref. [82], it was found that for a radiative natural SUSY model, where all contributions to the weak scale lie within the ABDS window, a relative probability $P_\mu \sim 1.4$ was computed whilst the SM, valid up to the reduced Planck mass m_P , had $P_\mu \sim 10^{-26}$. Also, split SUSY– with scalar masses at 10^6 TeV– had $P_\mu \sim 10^{-11}$. Other models such as CMSSM[83], PeV-SUSY[14], spread SUSY[84], minisplit[17], high-scale SUSY[85] and G_2MSSM [86] were also examined and found to have tiny values of P_μ . Thus, while the emergence of EW fine-tuned models is logically possible from the landscape, their likelihood is highly suppressed compared to natural models: natural SUSY models are much more plausible as a low energy effective field theory (LE-EFT) realization of the string landscape.

With the above considerations in mind, in this paper we first wish to explore in Sec. 2 the expectations for Higgs boson and sparticle masses from the nAMSB model with sequestered sector SUSY breaking– as might be expected from SUSY brane-world models, and as char-

acterized by the presence of bulk A -terms ($A_0 \neq 0$ but also including AMSB A -terms). The nAMSB0 model with $A_0 = 0$ has been shown in Fig. 2 of Ref. [64] to allow for naturalness ($\Delta_{EW} \lesssim 30$) but only if $m_h \lesssim 123$ GeV. With the string landscape in mind, we expect the various bulk soft terms and $m_{3/2}$ to be distributed as a power-law draw to large values in the multiverse as suggested by Douglas[87]. By combining the draw to large soft terms with the requirement of a weak scale within the ABDS window, then the putative distribution of Higgs and sparticle masses from the landscape may be derived in the context of those string models which reduce to a nAMSB low energy effective theory. Generically, under charged SUSY breaking with gravity-mediated scalar masses, we expect non-universality within different GUT multiplets and different generations, so we adopt independent masses $m_0(i)$, ($i = 1-3$ a generation index), along with $m_{H_u} \neq m_{H_d}$. Motivated by the fact that all members of each generation fill out a complete 16-d spinor of $SO(10)$, we maintain universality within each generation (as emphasized by Nilles *et al.*[88]). One issue is that the bulk trilinear soft terms A_0 are expected to be forbidden under charged SUSY breaking[14]. These results show the difficulty of deriving $m_h \sim 125$ GeV in such models without bulk A -terms. Thus, our ultimate parameter space is

$$m_0(i), m_{3/2}, A_0, \mu, m_A, \tan\beta \quad (nAMSB). \quad (9)$$

We then restrict ourselves to a set of string landscape vacua with the MSSM as the low energy EFT, but where gauginos gain AMSB masses, but the remaining soft terms scan within the multiverse and include bulk terms. (While soft terms are expected to be correlated within our universe, they may scan within the multiverse[89].)

With this setup in mind, the remainder of this paper is organized as follows. In Sec. 2, we assume a simple $n = +1$ power-law draw on soft terms in the landscape, and plot out probability functions for the various expected Higgs and sparticle masses for $nAMSB$ with $A_0 \neq 0$. These models can be natural whilst also respecting $m_h \sim 125$ GeV. In Sec. 3, we present several $AMSB$ benchmark points and model lines. In Sec. 4, we present sparticle production cross sections expected from nAMSB along our given model line. Here, we find that typically higgsino and wino pair production is dominant over the entire range of $m_{3/2}$ values. In Sec. 5, we discuss the wino decays in nAMSB for the dominantly produced sparticles. In Sec's 6, we discuss the main signal channels expected for LHC searches for nAMSB. Given the AMSB weak scale gaugino mass ratio $M_1 : M_2 : M_3 \sim 3 : 1 : 8$, it is possible that strong new limits on gaugino pair production from LHC could exclude $nAMSB$ up to and perhaps even beyond its naturalness limit. However, there remains a low mass window with $m(\text{wino}) \gtrsim m(\text{higgsino})$ which is still allowed due to the semi-compressed spectrum of the EWinos. After implementing present LHC constraints on nAMSB parameter space, in Sec. 7 we discuss the most favorable avenues for future SUSY searches within the nAMSB framework: via higgsino and wino pair production. Our summary and conclusions follow in Sec. 8.

2 Sparticle and Higgs masses in $nAMSB$ from the landscape

Here, we scan over parameters with a landscape-motivated m_{soft}^1 (linear) draw to large soft terms[87, 90]:

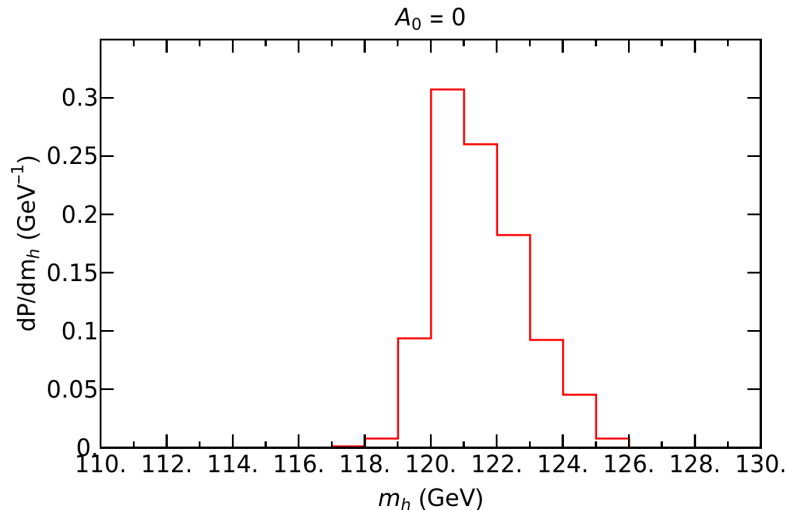


Figure 1: Plot of dP/dm_h from an $n = 1$ landscape scan in the nAMSB0 model where $A_0 = 0$.

- $m_{3/2} : 80 - 400$ TeV,
- $m_0(1, 2) : 1 - 20$ TeV,
- $m_0(3) : 1 - 10$ TeV,
- $A_0 : 0 - \pm 20$ TeV,
- $m_A : 0.25 - 10$ TeV,
- $\tan \beta : 3 - 60$ (flat scan).

In accord with naturalness, we fix $\mu = 250$ GeV. In lieu of requiring the pocket-universe value of m_Z^{PU} to lie within the ABDS window, we instead invoke $\Delta_{EW} < 30$ to avoid finetuning from terms beyond the ABDS window: the finetuned solutions are much more rare compared to non-finetuned (natural) solutions because in the finetuned case the scan parameter space rapidly shrinks to a tiny interval[80, 82]. For the present case, we restrict the landscape to those vacuum solutions which lead to the nAMSB model as the low energy effective field theory, but where the contributions to the soft breaking terms scan over this restricted portion of the multiverse.

Our first results are shown in Fig. 1 for the nAMSB0 model where A_0 is fixed at zero. In this case, we see that the probability distribution peaks at $m_h \sim 120$ GeV and falls sharply with increasing m_h . While some probability still exists for $m_h \sim 125$ GeV, we henceforth move beyond nAMSB0 to the nAMSB model with $A_0 \neq 0$ where prospects for generating a Higgs mass m_h in accord with LHC data are much better.

Our first results for nAMSB are shown in Fig. 2. In frame *a*), we show the differential probability distribution dP/dm_h vs. m_h , where P is the probability normalized to unity. The red histogram shows the full probability distribution while the blue-dashed histogram shows the same distribution after LHC sparticle mass limits (discussed in Sec. 6) are imposed. We

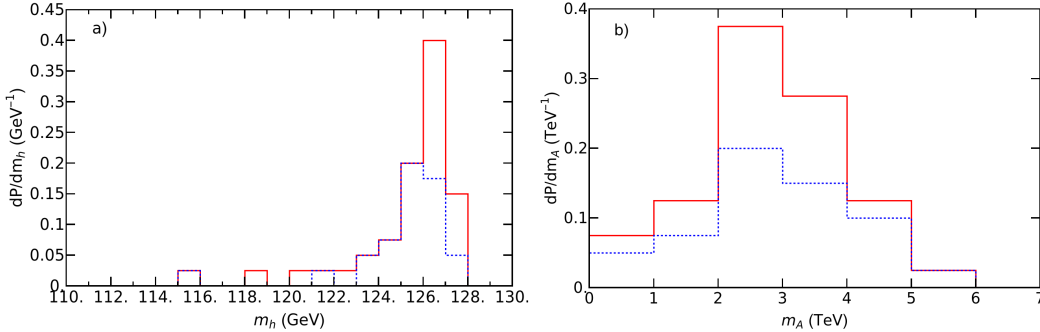


Figure 2: Plot of *a*) dP/dm_h and *b*) dP/dm_A , from an $n = 1$ landscape scan in the nAMSB model. The red histogram shows the full probability distribution while the blue-dashed histogram shows the remaining distribution after LHC sparticle mass limits are imposed.

see that dP/dm_h has only small values for $m_h \lesssim 123$ GeV, but then peaks sharply in the range $m_h \sim 125 - 127$ GeV. This is in accord with similar results in models with unified gaugino masses[90] or mirage-mediated gaugino masses[91]: basically, the soft terms $m_0(1,2)$, $m_0(3)$, A_0 , m_A and $m_{3/2}$ are selected to be as large as possible subject to the condition that the derived value of m_Z^{PU} lies within the ABDS window. This pulls the stop soft terms $m_0(3)$ large into the ~ 5 TeV range (but not too large) and also the bulk term A_0 to large- nearly maximal- mixing values, but not so large as to lead to CCB minima of the scalar potential (CCB or no-EWSB minima must be vetoed as not leading to a livable universe as we know it). These conditions pull m_h up to the vicinity of ~ 125 GeV. We also show in frame *b*) the distribution in pseudoscalar Higgs mass m_A , where m_A contributes directly to the weak scale through Eq. 7 since for $m_{H_d} \gg m_Z$, then $m_A \simeq m_{H_d}$ (and $m_H \sim m_{H^\pm} \sim m_A$). Here, we see that m_A reaches peak probability around ~ 2.5 TeV, somewhat beyond the reach of HL-LHC[92]. Maximally, m_A can extend up to ~ 6 TeV before overcontributing to the weak scale.

In Fig. 3, we show the probability for selected nAMSB model input parameters. In frame *a*), the distribution $dP/dm_{3/2}$ rises to a broad peak between $m_{3/2} : 100 - 250$ TeV and cuts off sharply around 300 TeV. The upper cutoff on $m_{3/2}$ occurs because as $m_{3/2} \rightarrow 300$ TeV, then $m_{\tilde{g}}$ is pulled beyond 5 - 6 TeV. In this case, the coupled RGEs pull stop masses so high that $\Sigma_u^u(\tilde{t}_{1,2})$ start contributing too much to the weak scale. In frame *b*), we show the distribution in first/second generation sfermion soft mass $m_0(1,2)$. Here, the distribution rises steadily to the scan upper limit since first/second generation sfermion contributions to the weak scale $\Sigma_u^u(\tilde{f}_{1,2})$ are proportional to the corresponding fermion Yukawa coupling. This pull to multi-TeV values of first/second generation squarks and sleptons provides a landscape amelioration of the SUSY flavor and CP problems[93]. We also show as a black-dashed histogram the results from a special run with increased upper scan limit of $m_0(1,2) < 50$ TeV. In this case, the distribution peaks at $m_0(1,2) \sim 15 - 30$ TeV before getting damped by the anthropic condition that m_Z^{PU} lies within the ABDS window. In frame *c*), we show the distribution in third generation soft term $m_0(3)$. In this case, the distribution peaks at ~ 5 TeV albeit with a distribution extending between 2 - 10 TeV. The reason for the upper cutoff is usually that the $\Sigma_u^u(\tilde{t}_{1,2})$ contribution to the weak scale becomes too large. Finally, in frame *d*), we show the distribution in the

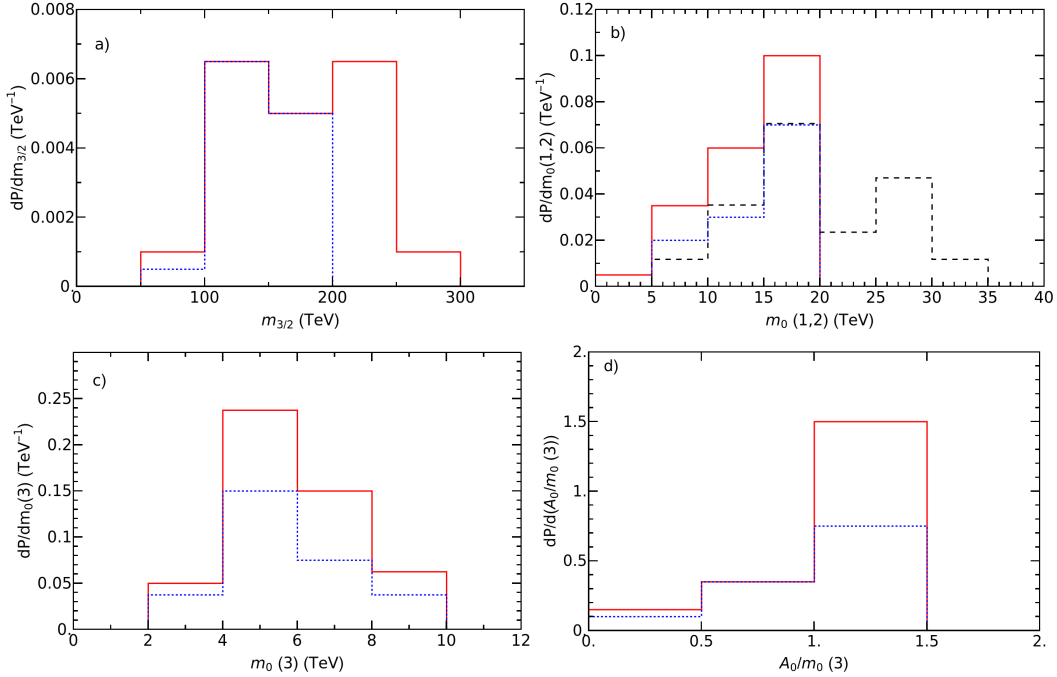


Figure 3: Plot of *a*) $dP/dm_{3/2}$, *b*) $dP/dm_0(1,2)$, *c*) $dP/dm_0(3)$ and *d*) $dP/d(A_0/m_0(3))$ from an $n = 1$ landscape scan in the nAMSB model. The red histogram shows the full probability distribution while the blue-dashed histogram shows the remaining distribution after LHC sparticle mass limits are imposed.

ratio $A_0/m_0(3)$. This distribution shows the prediction of large bulk A -terms which actually suppress the contributions of $\Sigma_u^u(\tilde{t}_{1,2})$ to the weak scale[56]. But if A_0 gets too big, then one is pulled into CCB vacua[94] which fail the anthropic criteria.

In Fig. 4, we show the $n = +1$ landscape probability distribution predictions for various sparticle masses. In frame *a*), we show the distribution in gluino mass $m_{\tilde{g}}$. The distribution begins around $m_{\tilde{g}} \sim 2$ TeV and peaks at $m_{\tilde{g}} \sim 3 - 4.5$ TeV. This “stringy natural”[95] distribution can explain why it was likely that LHC would not discover weak scale SUSY via gluino pair production at Run 2, and why gluino pair searches may even elude HL-LHC searches[96]. The light stop mass distribution is shown in frame *b*), and predicts $m_{\tilde{t}_1} \sim 1 - 2.5$ TeV which is mostly within range of HL-LHC[97]. In frame *c*), we show the distribution in $m_{\tilde{\chi}_2^\pm}$ which is approximately the wino mass. Here, the bulk of the probability distribution lies between $M_2 \sim 300 - 700$ GeV, making wino pair production an inviting target for LHC searches. In Fig. 4*d*), we show the distribution in mass difference of the two lightest neutralinos: $m_{\tilde{\chi}_2^0} - m_{\tilde{\chi}_1^0}$. This mass gap is relevant for the reaction $pp \rightarrow \tilde{\chi}_1^0 \tilde{\chi}_2^0$ where $\tilde{\chi}_2^0 \rightarrow f \tilde{f} \tilde{\chi}_1^0$ and thus provides a kinematic upper bound for the $m(f\tilde{f})$ invariant mass. From the distribution, the mass gap peaks between 10-15 GeV with a tail extending out to 40 GeV (and even beyond).

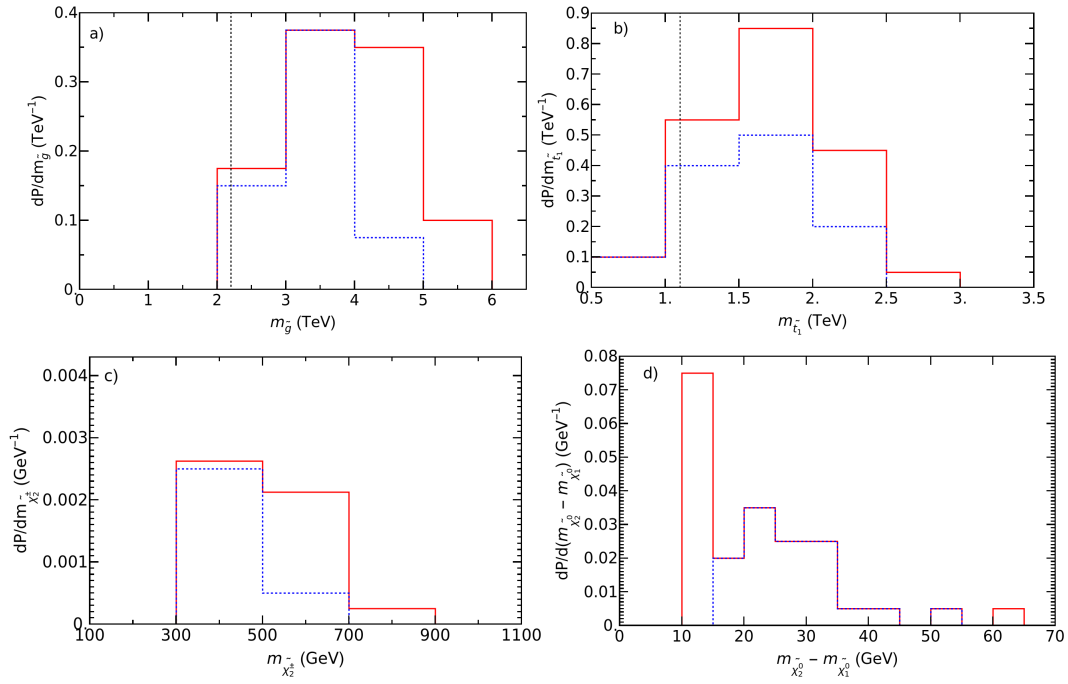


Figure 4: Plot of a) $dP/dm_{\tilde{g}}$, b) $dP/dm_{\tilde{t}_1}$, c) $dP/dm_{\tilde{\chi}_2^\pm}$ and d) $dP/d(m_{\tilde{\chi}_2^0} - m_{\tilde{\chi}_1^0})$ from an $n = 1$ landscape scan in the nAMSB model. The red histogram shows the full probability distribution while the blue-dashed histogram shows the remaining distribution after LHC particle mass limits are imposed.

3 *AMSB* benchmark points and model lines

In this Section, we compile three AMSB model benchmark points using the Isajet 7.91 code[98] for sparticle and Higgs mass spectra. The 7.91 version includes several fixes which give better convergence in the nAMSB model than previous versions.

3.1 *mAMSB*, *nAMSB0* and *nAMSB* benchmark points

3.1.1 *mAMSB* benchmark

In Table 1, we list three AMSB model benchmark points from three different AMSB models, but with similar underlying parameters which are convenient for comparison. In Column 2, we list sparticle and Higgs masses for the usual minimal AMSB model[48, 49] where universal bulk scalar contributions m_0^2 were added to all AMSB scalar soft masses but no bulk A_0 terms were included. We take $m_{3/2} = 125$ TeV and $\tan\beta = 10$ with $m_0 = 5$ TeV. The μ term is finetuned to a value $\mu = 1719$ GeV to ensure $m_Z = 91.2$ GeV, so the model will be highly finetuned with $\Delta_{EW} = 711$ (as listed). The gluino mass $m_{\tilde{g}} = 2.73$ TeV so that gluinos are safely beyond LHC Run 2 search limits which require $m_{\tilde{g}} \gtrsim 2.3$ TeV (in simplified models). The light Higgs mass $m_h = 120.3$ GeV: too light compared to its measured value (and so this BM point is ruled out). The LSP is wino-like with mass $m_{\tilde{\chi}_1^0} = 366$ GeV while $\tilde{\chi}_2^0$ is binolike and the $\tilde{\chi}_{3,4}^0$ and $\tilde{\chi}_2^\pm$ are higgsinolike with mass $\sim \mu$. The top-squark is not very mixed with $m_{\tilde{t}_1} = 3.43$ TeV, safely above LHC stop search limits. With a wino-like LSP, the thermally-produced relic abundance $\Omega_{\tilde{\chi}}^{TP} h^2 = 0.009$, underabundant by a factor ~ 13 . Thus, non-thermal wino production mechanisms would need to be active to fulfill the relic abundance with pure wino dark matter, which would then be ruled out by indirect WIMP detection experiments, where winos could annihilate strongly in dwarf galaxies, thus yielding high energy gamma rays in violation of limits[62] from Fermi-LAT and HESS. Alternatively, a tiny abundance of wino DM could be allowed if some other particle such as axions constituted the bulk of dark matter[63].

3.1.2 *nAMSB0* benchmark

Benchmark point nAMSB0 shows the expected sparticle and Higgs mass spectra from the generalized AMSB model inspired by DSB where hidden sector singlets are not allowed. This leads to allowed– but non-universal– scalar masses whilst gaugino masses and A -terms are suppressed and thus assume their loop-suppressed AMSB form. Thus, for nAMSB0 we adopt the parameter space Eq. 9 but with $A_0 = 0$. We adopt a natural value of $\mu = 250$ GeV with $m_A = 2$ TeV and also allow for higher first/second generation scalar masses as expected from the landscape, with $m_0(1, 2) = 10$ TeV whilst $m_0(3) = 5$ TeV as in the mAMSB benchmark point.

For nAMSB0, the natural value of $\mu = 250$ GeV implies light higgsinos so that while winos are still the lightest gauginos, the higgsinos are the lightest EWinos, and thus the expected phenomenology markedly changes from mAMSB. The small value of μ also makes the nAMSB0 model much more natural than mAMSB, where Δ_{EW} has dropped to 60. The dominant contributions to Δ_{EW} come now from $\Sigma_u^u(\tilde{t}_{1,2})$. But the model is still somewhat unnatural since the largest contribution to the RHS of Eq. 7 is still ~ 500 GeV, outside the ABDS window[81],

parameter	mAMSB	nAMSB0	nAMSB
$m_{3/2}$	125000	125000	125000
$\tan \beta$	10	10	10
$m_0(1, 2)$	5000	10000	10000
$m_0(3)$	5000	5000	5000
A_0	0	0	6000
μ	1718.8	250	250
m_A	5185.3	2000	2000
$m_{\tilde{g}}$	2728.1	2803.0	2802.4
$m_{\tilde{u}_L}$	5460.8	10211.8	10210.9
$m_{\tilde{u}_R}$	5484.4	10289.0	10312.1
$m_{\tilde{e}_R}$	4965.1	9918.6	9889.4
$m_{\tilde{t}_1}$	3428.4	3165.3	1487.9
$m_{\tilde{t}_2}$	4564.6	4253.6	3657.9
$m_{\tilde{b}_1}$	4545.6	4238.5	3691.4
$m_{\tilde{b}_2}$	5435.8	5239.3	5165.7
$m_{\tilde{\tau}_1}$	4918.6	4789.1	4692.3
$m_{\tilde{\tau}_2}$	4945.1	4253.6	4978.0
$m_{\tilde{\nu}_\tau}$	4945.7	4940.9	4956.6
$m_{\tilde{\chi}_2^\pm}$	1746.6	393.6	387.9
$m_{\tilde{\chi}_1^\pm}$	366.2	241.2	238.1
$m_{\tilde{\chi}_4^0}$	1745.2	1176.6	1174.2
$m_{\tilde{\chi}_3^0}$	1742.4	402.4	395.0
$m_{\tilde{\chi}_2^0}$	1163.0	260.9	260.4
$m_{\tilde{\chi}_1^0}$	366.0	229.4	226.3
m_h	120.3	120.7	125.0
$\Omega_{\tilde{\chi}_1^0}^{TP} h^2$	0.009	0.01	0.01
$BF(b \rightarrow s\gamma) \times 10^4$	3.1	3.2	3.3
$BF(B_s \rightarrow \mu^+\mu^-) \times 10^9$	3.8	3.8	3.8
$\sigma^{SI}(\tilde{\chi}_1^0, p)$ (pb)	7.5×10^{-11}	1.8×10^{-8}	1.6×10^{-8}
$\sigma^{SD}(\tilde{\chi}_1^0, p)$ (pb)	1.7×10^{-7}	2.2×10^{-4}	2.6×10^{-4}
$\langle \sigma v \rangle _{v \rightarrow 0}$ (cm ³ /sec)	6.1×10^{-25}	2.4×10^{-25}	2.6×10^{-25}
Δ_{EW}	711	60	15.0

Table 1: Input parameters and masses in GeV units for the mAMSB, nAMSB0 and nAMSB natural generalized anomaly mediation SUSY benchmark points with $m_t = 173.2$ GeV using Isajet 7.91.

and thus in need of finetuning. Another problem is the light Higgs mass $m_h = 120.7$ GeV. Both of these issues arise from the rather small AMSB0 value for the trilinear soft terms.

3.1.3 *n*AMSB benchmark

In the fourth column of Table 1, we list the *n*AMSB benchmark point which could arise from the sequestered SUSY breaking scenario of RS[23], where in addition to bulk scalar masses, bulk A -terms are also expected. Here, we use the same parameters as in *n*AMSB0 except now also allow $A_0 = 6$ TeV. The large trilinear soft term leads to large stop mixing which feeds into the m_h value (which is maximal for stop mixing parameter $x_t \sim \sqrt{6}m_{\tilde{t}}$) so that now the value of m_h is lifted to 125 GeV in accord with LHC measurements. Also, the large positive A -term leads to cancellations in both of $\Sigma_u^u(\tilde{t}_1)$ and $\Sigma_u^u(\tilde{t}_2)$ leading to increased naturalness where now $\Delta_{EW} = 15$. For the *n*AMSB0 benchmark, the more-mixed lighter stop mass has dropped to just $m_{\tilde{t}_1} \sim 1.5$ TeV, within striking distance of HL-LHC[97].

3.2 Corresponding AMSB model lines

In this Subsection, we elevate each of the AMSB benchmark points to AMSB model lines where we keep the auxiliary parameters fixed as before but now allow the fundamental AMSB parameter $m_{3/2}$ to vary. We compute the AMSB model line spectra using Isasugra.

In Fig. 5, we first show the naturalness measure Δ_{EW} for each model line. For the *m*AMSB model line, we see that Δ_{EW} starts at ~ 100 for low $m_{3/2} \sim 50$ TeV, and then steadily increases to $\Delta_{EW} \sim 10^4$ for $m_{3/2} \sim 500$ TeV. As for the *m*AMSB BM point, the dominant contribution to Δ_{EW} comes from the (finetuned) μ parameter. This model line thus seems highly implausible for all $m_{3/2}$ values based on naturalness. We also show the *n*AMSB0 model line as the orange curve. Here, Δ_{EW} ranges from 50 – 200 as $m_{3/2}$ varies over 50 – 500 TeV. While more natural than *m*AMSB, it still lies outside the ABDS window which is typified by $\Delta_{EW} \lesssim 30$. The blue curve shows the *n*AMSB model line. In this case, Δ_{EW} ranges from $\sim 15 - 150$. The line $\Delta_{EW} = 30$ is shown by the dashed red curve. Here, we see the model line starts becoming unnatural for $m_{3/2} \gtrsim 265$ TeV.

In Fig. 6, we show the computed value of m_h along the three model lines. The LHC measured window is between $m_h : 123 - 127$ allowing for a ± 2 GeV theory error in the computed value of m_h . We see that the *m*AMSB model line enters the allowed region of m_h only for $m_{3/2} \gtrsim 400$ TeV while the *n*AMSB0 model line enters the allowed m_h range for $m_{3/2} \gtrsim 300$ TeV. Both model lines are highly unnatural for such large $m_{3/2}$ values. However, the *n*AMSB model line is within the $m_h = 125 \pm 2$ GeV band for $m_{3/2} : 50 - 280$ TeV, consistent with its natural allowed range (thanks to the presence of bulk A_0 terms).

In Fig. 7, we show various sparticle masses for the *n*AMSB model line vs. $m_{3/2}$. The dark and light blue and lavender lines show the various higgsino-like EWinos which are typically of order $m(\text{higgsinos}) \sim \mu \sim 250$ GeV. Next heaviest are the wino-like EWinos $\tilde{\chi}_3^0$ and $\tilde{\chi}_2^\pm$, shown as green and orange curves. These masses vary from $m(\text{winos}) : 300 - 2000$ GeV over the range of $m_{3/2}$ shown, and are, as we shall see, subject to present and future LHC EWino searches.

The black curve shows the gluino mass $m_{\tilde{g}} : 1.2 - 10$ TeV. We also show the LHC lower

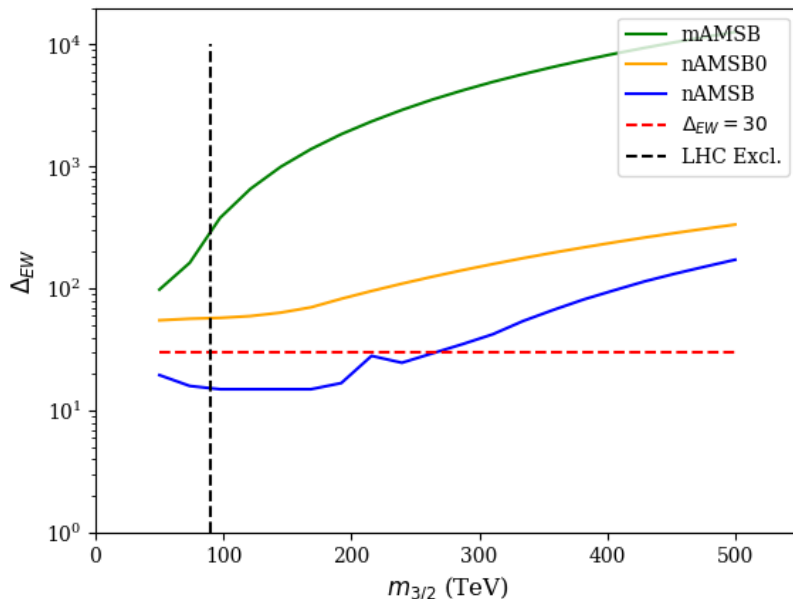


Figure 5: Plot of Δ_{EW} vs. $m_{3/2}$ along the AMSB model lines. The region below the dashed line $\Delta_{EW} < 30$ is regarded as natural.

bound $m_{\tilde{g}} \sim 2.3$ TeV from gluino pair searches within the context of simplified models by the black dashed line. The LHC simplified model results should apply well in the case of nAMSB models since the $\tilde{g} - \tilde{\chi}_1^0$ mass gap is always substantial. The LHC $pp \rightarrow \tilde{g}\tilde{g}X$ search limits thus provide a lower bound on allowed nAMSB parameter space with $m_{3/2} \gtrsim 90$ TeV. The blue dashed line denotes the upper limit on $m_{3/2}$ obtained from naturalness constraints. The lighter top squark mass $m_{\tilde{t}_1}$ is also shown, and is beyond the LHC simplified model limit $m_{\tilde{t}_1} \gtrsim 1.1$ TeV for all $m_{3/2}$ values. First/second generation sfermion masses lie around $m_0(1, 2)$ value so in this case would be inaccessible to present and future LHC searches. By combining lower limits from LHC gluino pair searches with upper bounds from naturalness, we expect the allowed $m_{3/2}$ values for nAMSB to lie between $m_{3/2} : 90 - 265$ TeV.

4 LHC production cross sections

In this Section, we pivot to prospects for LHC searches for SUSY within the context of the nAMSB model. First, we adopt the computer code PROSPINO[99] to compute the NLO production cross sections for various $pp \rightarrow SUSY$ reactions, given input from the Isajet SUSY Les Houches Accord (SLHA) file[100]. Our first results are shown in Fig. 8 where we show cross sections for $pp \rightarrow \tilde{g}\tilde{g}, \tilde{t}_1\tilde{t}_1^*$ and (summed) EWino pair production vs. $m_{3/2}$ along the nAMSB model line. At the top of the plot, we see EWino pair production is dominant and relatively flat vs. $m_{3/2}$ since it is dominated by higgsino pair production and μ is fixed at 250 GeV. The EWino cross section are divided up into summed $\tilde{\chi}_i^0\tilde{\chi}_j^0, \tilde{\chi}_i^0\tilde{\chi}_k^\pm$ and $\tilde{\chi}_k^\pm\tilde{\chi}_l^\mp$ production, where

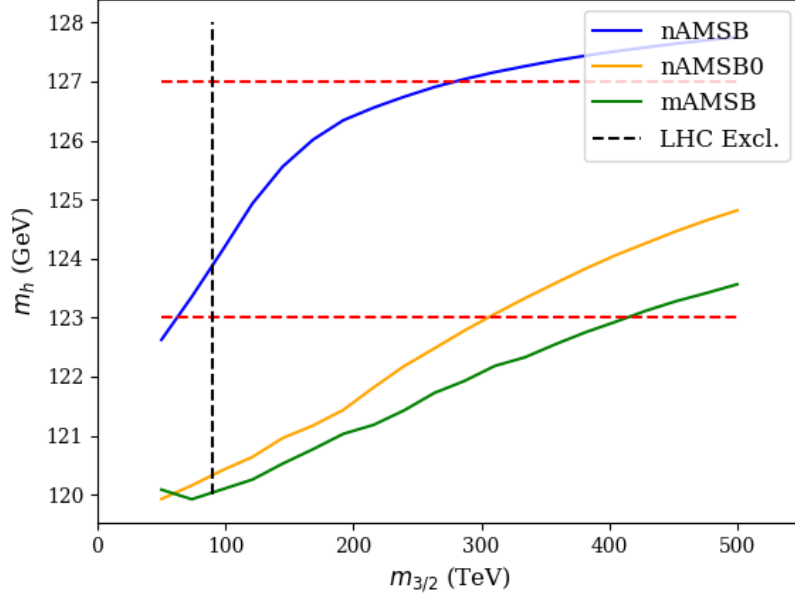


Figure 6: Plot of m_h vs. $m_{3/2}$ along the AMSB model lines. The light Higgs mass is constrained by LHC measurements to lie between the dashed lines, given some theory error on the calculation of m_h .

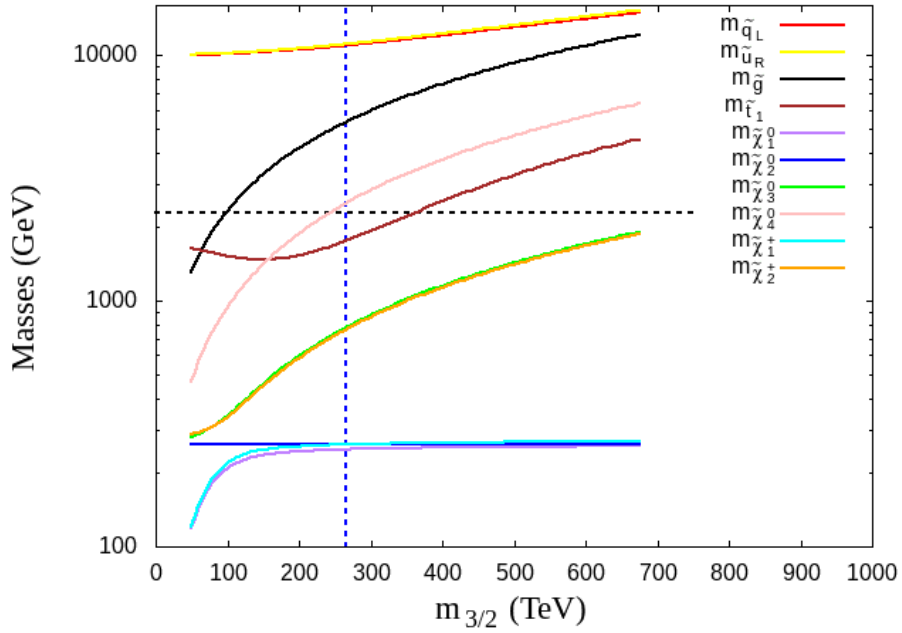


Figure 7: Plot of sparticle masses vs. $m_{3/2}$ along the nAMSB model lines.

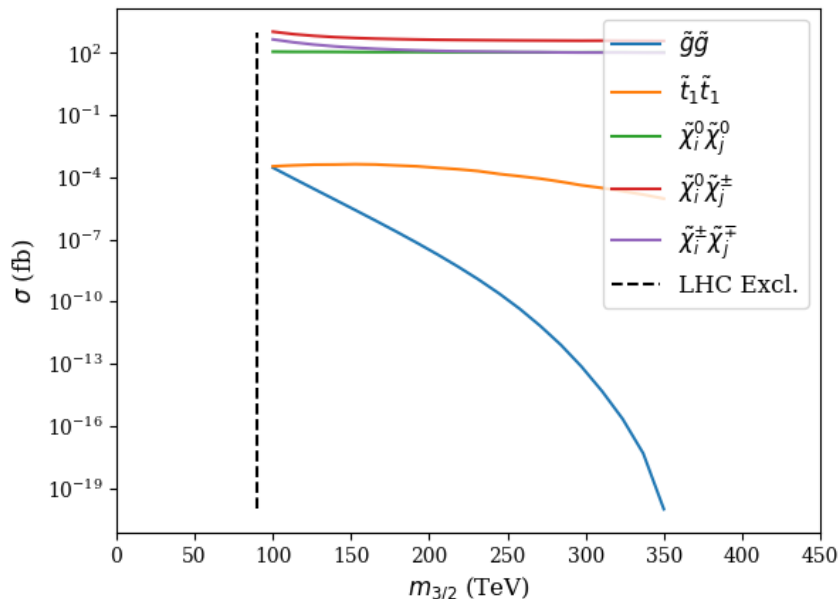


Figure 8: Plot of $\sigma(pp \rightarrow \tilde{g}\tilde{g}, \tilde{t}_1\tilde{t}_1^*)$ and EWino pair production vs. $m_{3/2}$ along the nAMSB model line.

$i, j = 1 - 4$ and $k, l = 1 - 2$. The summed EWino pair cross sections are all comparable and of order $\sim 10^2$ fb. The $pp \rightarrow \tilde{t}_1\tilde{t}_1^*$ cross section is also relatively flat, this time reflecting that $m_{\tilde{t}_1}$ hardly changes with increasing $m_{3/2}$ (from Fig. 7). The $pp \rightarrow \tilde{g}\tilde{g}$ cross section is falling rapidly with increasing $m_{3/2}$, reflecting that the gluino mass is directly proportional to $m_{3/2}$. From the plot, we thus expect most of the reach of LHC for the nAMSB model will come from EWino pair production rather than from gluino or stop pair production.

There are many subreactions that contribute to the summed EWino pair production cross sections. Each subreaction leads to different final states and thus different SUSY search strategies. In Fig. 9a), we show the several chargino-chargino pair production reactions vs. $m_{3/2}$. The upper blue curve denotes $\tilde{\chi}_1^+\tilde{\chi}_1^-$ where the light charginos are mainly higgsino-like (except for some substantial mixing at low $m_{3/2}$ where the wino soft term $M_2 \sim \mu$). Given the small $m_{\tilde{\chi}_1^+} - m_{\tilde{\chi}_1^0}$ mass gap, where much of the reaction energy goes into the invisible LSP mass and energy, this reaction is likely to be largely invisible at LHC. The orange curve denotes charged wino pair production: $\tilde{\chi}_2^+\tilde{\chi}_2^-$. Given its modest size and the branching fractions from Sec. 5, it can be very promising for LHC searches. The third reaction, mixed higgsino-wino $\tilde{\chi}_1^\pm\tilde{\chi}_2^\mp$ production, occurs at much lower rates.

In Fig. 9b), we show the ten neutralino pair production reactions $\sigma(pp \rightarrow \tilde{\chi}_i^0\tilde{\chi}_j^0)$. By far, the dominant neutralino pair production reaction is $pp \rightarrow \tilde{\chi}_1^0\tilde{\chi}_2^0$. This reaction takes place dominantly via s -channel Z^* exchange involving the coupling W_{ij} of Eq. 8.101 of Ref. [101]. The signs of the neutralino mixing elements add constructively in this case leading to a large higgsino pair production reaction that leads to promising LHC signature in the soft opposite-

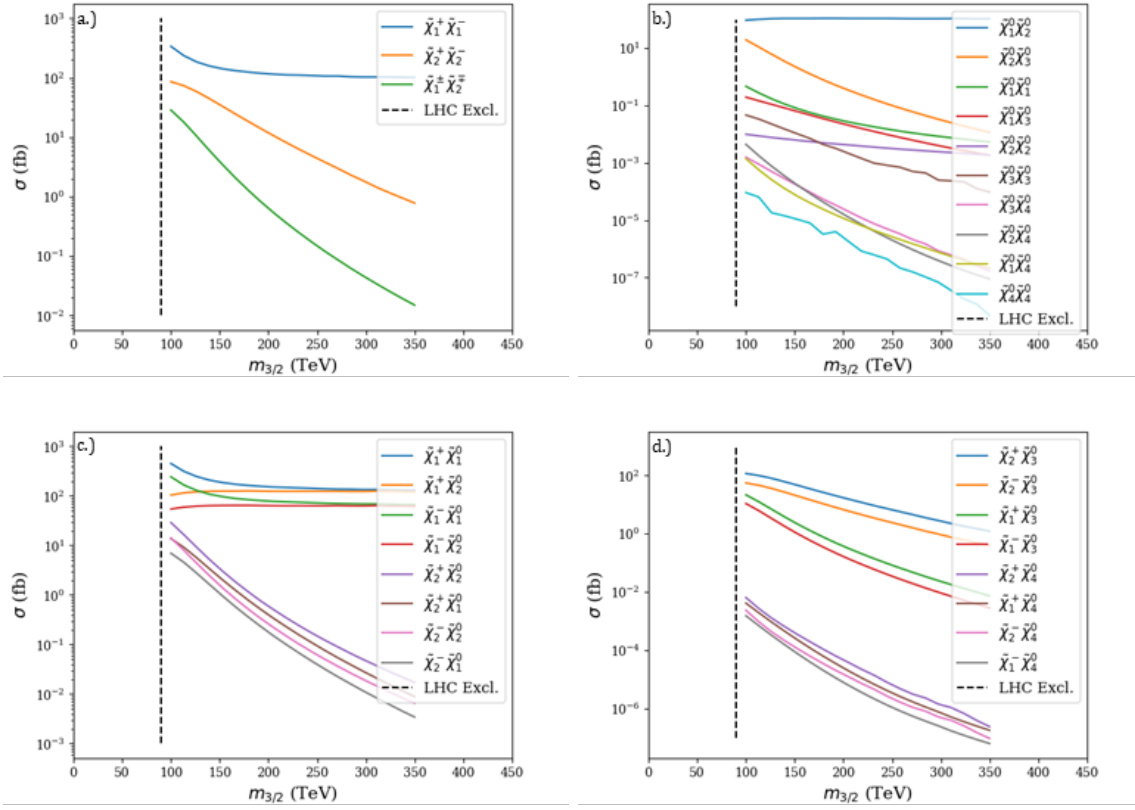


Figure 9: Plot of various EWino pair production cross sections vs. $m_{3/2}$ along the nAMSB model line: *a*) chargino pair production, *b*) neutralino pair production, *c*) chargino- $\tilde{\chi}_{12}^0$ pair production and *d*) chargino- $\tilde{\chi}_{3,4}^0$ pair production.

sign dilepton plus jets plus \cancel{E}_T channel[102, 103] (OSDLJMET). This cross section is flat with increasing $m_{3/2}$ since μ is not a soft term and not expected to directly scan in the landscape, but instead is fixed by whatever solution to the SUSY μ problem attains[104]. The next largest neutralino pair production cross section is $pp \rightarrow \tilde{\chi}_2^0 \tilde{\chi}_3^0$: wino-higgsino production, which again has a constructive sign interference along with large mixing terms. Other neutralino pair production reactions are subdominant and typically decreasing with increasing $m_{3/2}$.

In Fig. 9c), we show $\tilde{\chi}_{1,2}^0 \tilde{\chi}_k^\pm$ pair production reactions. The largest, $\tilde{\chi}_1^0 \tilde{\chi}_1^+$, may again be largely invisible to LHC searches while the second largest $\tilde{\chi}_2^0 \tilde{\chi}_1^+$ can contribute to the OSDLJMET signature mentioned above. The corresponding reactions with negative charginos are comparable to these reactions but somewhat suppressed since they occur mainly via s -channel W^* production and LHC is a pp collider which favors positively charged W bosons. The remaining higgsino-wino production reactions fall with increasing $m_{3/2}$ and are subdominant.

In Fig. 9d), we show the $\tilde{\chi}_{3,4}^0 \tilde{\chi}_k^\pm$ production rates. In this case, wino pair production $\tilde{\chi}_3^0 \tilde{\chi}_2^+$ is dominant but falling as $m_{3/2}$ —and hence M_2 —increases in value. The conjugate reaction $\tilde{\chi}_3^0 \tilde{\chi}_2^-$ reaction is next largest, followed by $\tilde{\chi}_3^0 \tilde{\chi}_1^\pm$. The reactions involving bino production $\tilde{\chi}_4^0$ are all subdominant and may not be so relevant for LHC SUSY searches.

5 Sparticle decay modes

In this Section, we wish to comment on some relevant sparticle branching fractions leading to favorable final state search signatures for LHC. It is evident from the preceding Section that EWino pair production is the dominant sparticle production mechanism at LHC14. The reaction $pp \rightarrow \tilde{\chi}_1^0 \tilde{\chi}_2^0$ (neutral higgsino pair production) is dominant, where $\tilde{\chi}_2^0 \rightarrow f \bar{f} \tilde{\chi}_1^0$ and where the f are SM fermions. For the case of nAMSB, the mass gap $m_{\tilde{\chi}_2^0} - m_{\tilde{\chi}_1^0}$ can range up to 50-60 GeV when winos are light, leading to substantial wino-higgsino mixing for lower values of $m_{3/2} \sim 100$ TeV. The lucrative leptonic branching fraction $\tilde{\chi}_2^0 \rightarrow \ell^+ \ell^- \tilde{\chi}_1^0$ occurs typically at the 2% level due to competition with other decay modes such as $\tilde{\chi}_2^0 \rightarrow \tilde{\chi}_1^\pm f \bar{f}'$.

The other lucrative production mode from the previous Section is wino pair production $pp \rightarrow \tilde{\chi}_3^0 \tilde{\chi}_2^\pm$. To assess the expected final states from this reaction, we plot in Fig. 10 the major wino decay branching fractions along the nAMSB model line. In frame *a*), we plot the $BF(\tilde{\chi}_2^+)$ values vs. $m_{3/2}$ while in frame *b*) we plot the $BF(\tilde{\chi}_3^0)$ values. From frame *a*), the region with $m_{3/2} \lesssim 90$ TeV is already excluded by LHC $\tilde{g}\tilde{g}$ searches (albeit in the context of simplified models). Below 90 TeV, there is actually a level-crossing: since μ is fixed at 250 GeV, a low enough value of $m_{3/2}$ leads to $m(\text{wino}) < m(\text{higgsino})$ and an *increased* $m_{\tilde{\chi}_2^+} - m_{\tilde{\chi}_1^+}$ mass gap (see Fig. 7) so that $\tilde{\chi}_2^+ \rightarrow \tilde{\chi}_1^+ h$ is allowed. Then, as $m_{3/2}$ increases, the mass gap drops (due to wino-higgsino degeneracy) and the $\tilde{\chi}_2^+ \rightarrow \tilde{\chi}_1^+ h$ mode becomes kinematically closed. As $m_{3/2}$ increases beyond ~ 100 TeV, then $\tilde{\chi}_2^+$ becomes wino-like, and the mass gap enlarges so that the decay $\tilde{\chi}_2^+ \rightarrow \tilde{\chi}_1^+ h$ becomes allowed again. As $m_{3/2}$ increases further, then all four decay modes $\tilde{\chi}_2^+ \rightarrow \tilde{\chi}_1^0 W^+$, $\tilde{\chi}_2^0 W^+$, $\tilde{\chi}_1^+ Z$ and $\tilde{\chi}_1^+ h$ asymptote to $\sim 25\%$. Thus, we expect the charged wino to decay to higgsino plus W , Z or h in a ratio $\sim 2 : 1 : 1$. Since the higgsinos may be quasi-visible (depending on decay mode and mass gap), then we get wino decay to W , Z or h +quasi-visible higgsinos as a final state.

In Fig. 10b), we show the neutral wino $\tilde{\chi}_3^0$ branching fractions along the nAMSB model

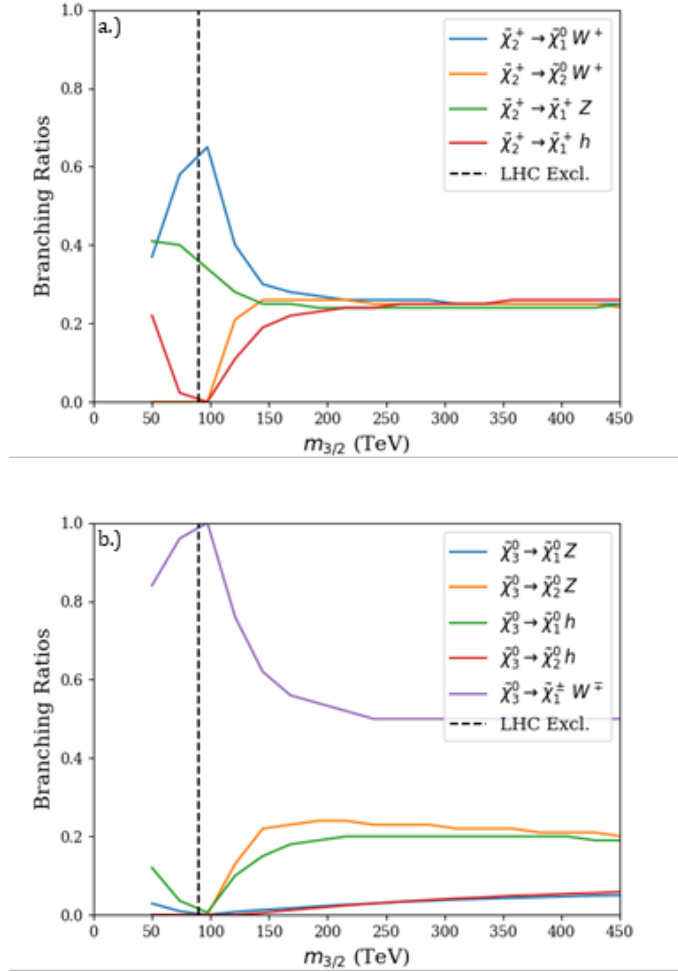


Figure 10: Plot of charged and neutral wino branching fractions *a*) $\text{BF}(\tilde{\chi}_2^+)$ and *b*) $\text{BF}(\tilde{\chi}_3^0)$ versus $m_{3/2}$ along the nAMSB model line.

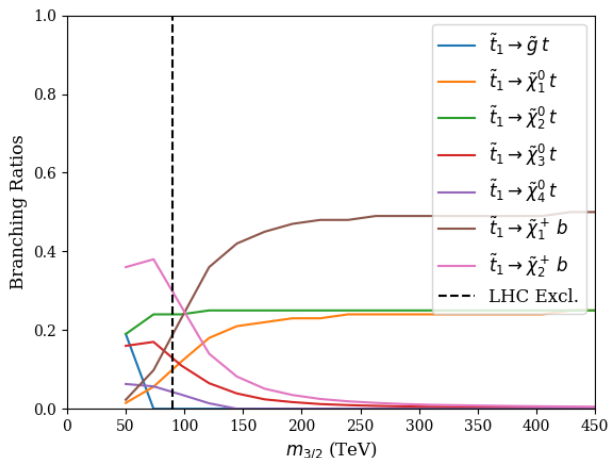


Figure 11: Plot of top squark branching fractions $BF(\tilde{t}_1)$ versus $m_{3/2}$ along the nAMSB model line.

line. At low $m_{3/2} \sim 90$ TeV near the LHC-excluded region, the neutral winos decay nearly 100% into $\tilde{\chi}_1^\mp W^\pm$. As $m_{3/2}$ increases, the wino-higgsino mass gap increases, and decays to $\tilde{\chi}_2^0 Z$ and $\tilde{\chi}_1^0 h$ are allowed and can occur at the $\sim 20\%$ level while decays to $\tilde{\chi}_1^\mp W^\pm$ asymptote to $\sim 50\%$. The remaining branching fraction goes to mixing-suppressed modes. Thus, for wino pair production, we expect a final state of $VV + MET$, $Vh + MET$ and $hh + MET$ where MET stands for missing transverse energy and V stands for the vector bosons W and Z . The MET may not really be entirely missing since it may include 3-body decay products of the heavier higgsinos.

In Fig. 11, we plot the light top squark branching fractions $BF(\tilde{t}_1)$ vs. $m_{3/2}$ along the nAMSB model line. For very low $m_{3/2}$, $\tilde{t}_1 \rightarrow b\tilde{\chi}_2^+$ is dominant where the $\tilde{\chi}_2^\pm$ is mixed wino-higgsino. But as $m_{3/2}$ increases, $BF(\tilde{t}_1 \rightarrow b\tilde{\chi}_1^+)$ becomes dominant and approaches 50%, not unlike natural SUSY models with gaugino mass unification[105]. The \tilde{t}_1 in nAMSB (as in NUHM2 models) is dominantly $\sim \tilde{t}_R$ in spite of large stop mixing soft term A_t . Also, at larger $m_{3/2}$ values, $BF(\tilde{t}_1 \rightarrow t\tilde{\chi}_{1,2}^0)$ each approach $\sim 25\%$.

6 LHC excluded regions

Certain regions of nAMSB model parameter space seem already excluded by existing LHC13 search limits from Run 2 with $\sim 139 \text{ fb}^{-1}$ of integrated luminosity.

6.1 LHC constraint from gluino pair searches

In the case of gluino pair production, for the bulk of LHC-allowed nAMSB parameter space, we expect $\tilde{g} \rightarrow t\tilde{t}_1^*$ followed by further \tilde{t}_1 cascade decays. The approximate ATLAS and CMS simplified model limits for $\tilde{g}\tilde{g}$ production followed by decay to third generation particles should

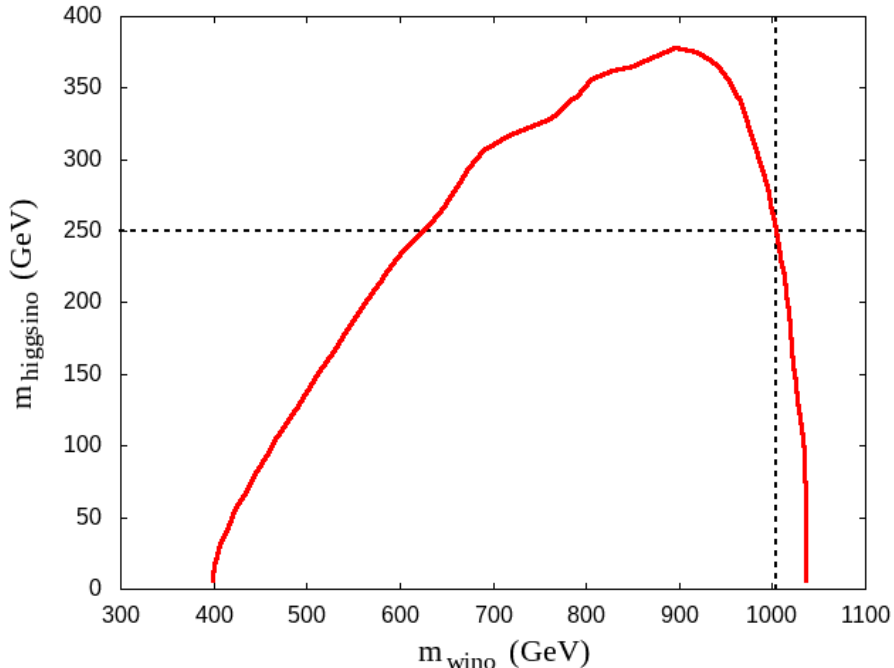


Figure 12: Allowed/excluded regions of $m(\text{wino})$ vs. $m(\text{higgsino})$ plane from ATLAS analysis of EWino pair production followed by decay to W, Z, h with decay to boosted dijets.

roughly apply[106, 107, 108], and these imply

$$m_{\tilde{g}} \gtrsim 2.3 \text{ TeV}. \quad (10)$$

From Fig. 7, this implies that $m_{3/2} \gtrsim 90 \text{ TeV}$.

6.2 LHC constraint from EWino pair production followed by decay to boosted dijets

A recent ATLAS study[109] reports searching for EWino pair production followed by two-body decays to W, Z or h . These heavy SM objects are assumed to decay hadronically to boosted dijet/fat-jet states which are then identified. A similar study by CMS was also made[110], but with smaller parameter space exclusion regions. The simplified model limits presented in Fig. 14c) of Ref. [109] should roughly apply to our case for wino-pair production $pp \rightarrow \tilde{\chi}_2^\pm \tilde{\chi}_3^0$ as shown in Fig. 9d) followed by decays to vector bosons and Higgs bosons as shown in Fig. 10. The digitized ATLAS exclusion curve is shown in Fig. 12 in the $m(\text{wino})$ vs. $m(\text{higgsino})$ plane. Our nAMSB model line with $\mu = 250 \text{ GeV}$ is denoted by the horizontal dashed line. From the plot, we would expect that the range $m(\text{wino}) : 625 - 1000 \text{ GeV}$ would be ruled out, corresponding to a range of $m_{3/2} : 200 - 350 \text{ TeV}$. For model lines with larger or smaller values of μ , the exclusion region changes accordingly in Fig. 12.

6.3 LHC constraints from SModelS/CheckMATE2 analysis

To test for further limits on nAMSB parameter space, we employ two recent recasting softwares: **SModelS**[111, 112, 113] and **CheckMATE2** (CM2)[114, 115] to study the impact of the current searches on nAMSB parameter space. **SModelS** is a popular tool for interpreting simplified-model results from the LHC. It decomposes Beyond the Standard Model (BSM) collider signatures presenting a Z_2 -like symmetry into Simplified Model Spectrum (SMS) topologies and compares the BSM predictions for the LHC in a model independent framework with the relevant experimental constraints. The main variable for comparison of a BSM theory to the LHC experimental searches is the r -ratio which is defined as the ratio of the expected $\sigma \times BR$ for a specific final state to the corresponding upper limit on the $\sigma \times BR \times \epsilon$ (where ϵ is the acceptance efficiency provided by the experimental paper). **CheckMATE2** is a reinterpretation software for interpreting LHC results for all BSM models. It is based on recasting the full experimental analyses using events after full Monte Carlo simulation, hadronization and detector smearing of the final state objects and implementing the cuts as in the experimental analyses. It provides the r value defined as the ratio of the expected number of events from the signal, after implementing all cuts, to the 95%CL upper limit from the experimental result. In both cases, for a BSM model to be allowed by current constraints, one requires $r < 1$.

The wino-higgsino mass gap, quantified by $\Delta m_{31} = m_{\tilde{\chi}_3^0} - m_{\tilde{\chi}_1^0}$, increases with $m_{3/2}$ as seen in Fig. 13. Fig. 14 shows the variation of the highest r value obtained from **SModelS** and **CheckMATE2** for the $\sqrt{s} = 13$ TeV results from LHC. The highest r -value defined as the ratio of the signal over the 95%CL upper limit from the signal region is plotted against $m_{3/2}$. The red dotted lines denote the constraints from the ATLAS search of boosted hadronically decaying bosons + \cancel{E}_T [109] while the black dotted line denote the bound from the gluino searches implying $m_{3/2} \geq 90$ TeV as discussed in Section 6.2 and 6.1 respectively.

For the constraints from the **CheckMATE2** CMS results (blue), we observe the tightest constraints arise from the multi-lepton (2/3) + \cancel{E}_T searches[116] for $m_{3/2} \sim 150$ TeV with r -value ~ 0.15 and it falls off on either side of the peak. This is due to other searches gaining more importance such as searches for $\geq 4\ell + \cancel{E}_T$ for larger mass-gaps between the wino-like and higgsino-like neutralino. From the **CheckMATE2** ATLAS result (green), the r -value decreases with increasing $m_{3/2}$ from $r = 0.25$ arising from the hadronic searches of squarks and gluinos [117].

From **SModelS** (red), the most stringent constraint occurs at $m_{3/2} < 100$ TeV from searches of three leptons + \cancel{E}_T [118]. For $m_{3/2} = 100 - 250$ TeV range, the most stringent constraints arise from the boosted hadronically decaying diboson + \cancel{E}_T searches the multi-lepton searches involving two or three leptons+ \cancel{E}_T [119, 118] are the most sensitive searches near the peak at $m_{3/2} \sim 225$ TeV. For higher $m_{3/2} = 250 - 400$ TeV, the dominant constraints arise from the multi-lepton searches and sub dominant constraints arise from the boosted hadronically decaying dibosons + \cancel{E}_T . As $m_{3/2}$ increases, the multijet + \cancel{E}_T [120] searches start constraining the parameter space dominantly. However, the r -value always remains less than 1: thus, the remaining allowed range of $m_{3/2} \sim 90 - 200$ TeV appears to be presently allowed.

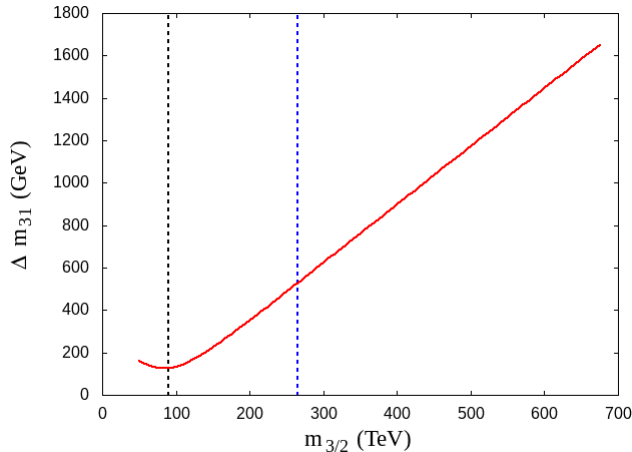


Figure 13: Variation of $\Delta m_{31} = m_{\tilde{\chi}_3^0} - m_{\tilde{\chi}_1^0}$ vs. $m_{3/2}$. The region left of the black-dashed curve is excluded by LHC13 gluino pair searches and the region to the right of the blue-dashed line is unnatural with $\Delta_{EW} \gtrsim 30$.

6.4 LHC-allowed nAMSB parameter space

Our final allowed nAMSB model line parameter space is shown in Fig. 15. The left gray shaded region is excluded by LHC gluino search limits while the central gray shaded region is excluded by the ATLAS limits on EWino pair production followed by decay to two boosted dijet final states. The naturalness limit is denoted by the vertical dashed line within the central excluded band: the region to the right is unnatural, and thus highly unlikely (but not impossible) to emerge from the landscape. The unshaded region extends from $m_{3/2} : 90 - 200$ TeV and is thus the presently allowed parameter space. For convenience, we display again the sparticle masses along our nAMSB model line. The remaining SUSY particle spectrum for $m_{3/2} \sim 90 - 200$ TeV should provide a target for future LHC searches seeking to discover or to rule out natural AMSB.

7 Prospects for nAMSB at Run3 and Hi-Lumi LHC searches

7.1 LHC higgsino pair production search

7.1.1 Soft opposite-sign dilepton, jet+MET search

In models with light higgsinos, as in natural SUSY, a compelling LHC search reaction[121] is $pp \rightarrow \tilde{\chi}_1^0 \tilde{\chi}_2^0$ followed by $\tilde{\chi}_2^0 \rightarrow \ell^+ \ell^- \tilde{\chi}_1^0$, where the dilepton pair is energetically rather soft since its invariant mass is kinematically bounded by $m_{\tilde{\chi}_2^0} - m_{\tilde{\chi}_1^0}$. By triggering on hard initial state QCD radiation[102, 103], then such soft dilepton + \cancel{E}_T events can be searched for at LHC. Prospects for soft dileptons, jets + \cancel{E}_T events (soft OSDLJMET) at LHC have been presented

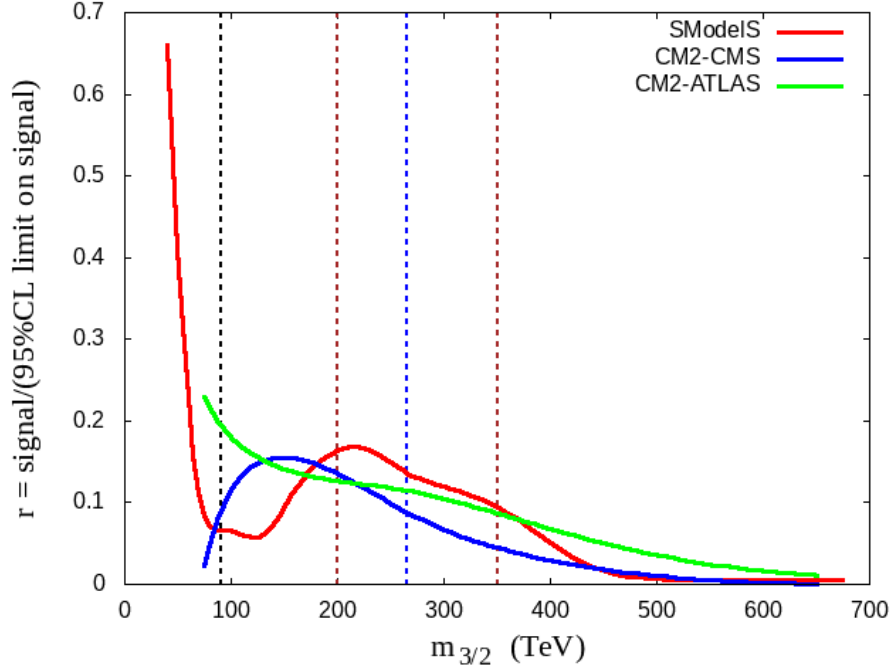


Figure 14: Plot of r from `SModelS` and `CheckMate2` vs. $m_{3/2}$ along the nAMSB model line.

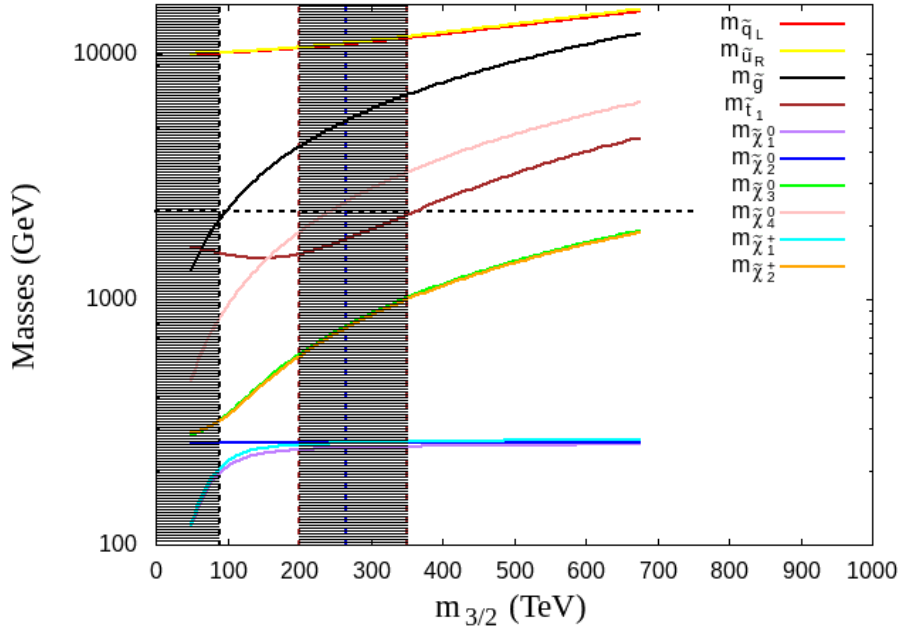


Figure 15: Allowed/excluded regions of our nAMSB model-line along with various sparticle masses.

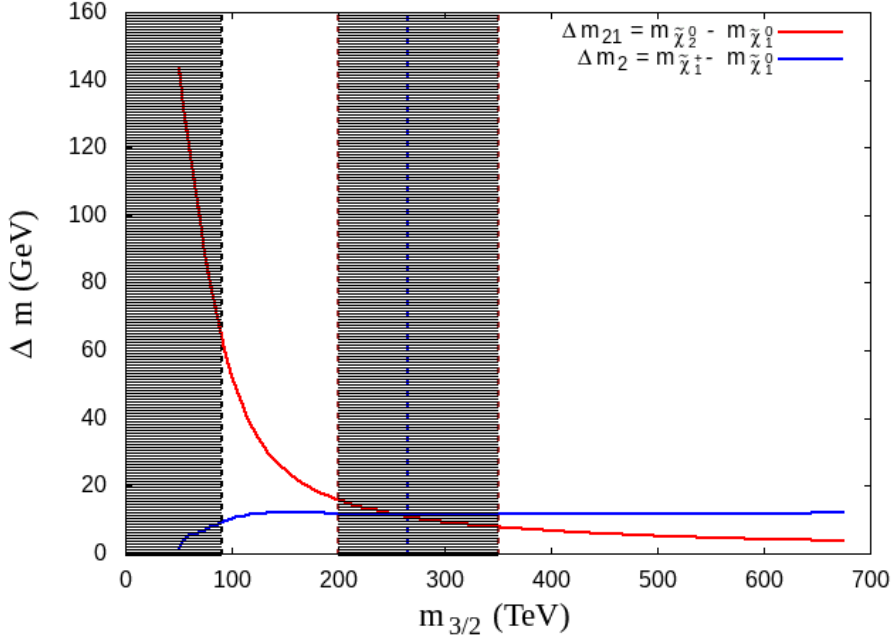


Figure 16: Plot of $m_{\tilde{\chi}_2^0} - m_{\tilde{\chi}_1^0}$ and $m_{\tilde{\chi}_1^+} - m_{\tilde{\chi}_1^0}$ mass gaps vs. $m_{3/2}$ along the nAMSB model line.

in the higgsino discovery plane[122] and in Ref. [123] where new angular cuts were proposed to aid in discovery. Recent search results from CMS[119] and ATLAS[124] have been presented.

The soft OSDJMET signal is a particularly compelling signal for SUSY in the nAMSB model in light of the large $pp \rightarrow \tilde{\chi}_1^0 \tilde{\chi}_2^0$ cross section from Fig. 9b). A distinguishing feature of the nAMSB model compared to models with gaugino mass unification or mirage mediation is the relatively larger $\Delta m_{21} \equiv m_{\tilde{\chi}_2^0} - m_{\tilde{\chi}_1^0}$ mass gap ranging from $\sim 15 - 60$ GeV for nAMSB as shown in Fig. 16 (due to the larger wino-higgsino mixing from light winos). Current searches from CMS and ATLAS probe a maximal μ value of ~ 200 GeV for mass gaps $\Delta m_{21} \sim 10$ GeV. Future ATLAS and CMS probes at HL-LHC with 3000 fb^{-1} can probe to $\mu \sim 300$ GeV[125] and the improved angular cuts may allow HL-LHC to probe as high as $\mu \sim 325$ GeV[123]. It should be noted that both ATLAS and CMS seem to have a 2σ excess in this channel at present with 139 fb^{-1} of integrated luminosity. In nAMSB with a larger $m_{\tilde{\chi}_1^+} - m_{\tilde{\chi}_1^0}$ mass gap, soft trilepton plus jet+ \cancel{E}_T signatures should also be available from $\tilde{\chi}_1^\pm \tilde{\chi}_2^0$ production.

7.2 LHC wino pair production search

7.2.1 Boosted hadronic signature

The rather light winos expected from the allowed parameter-space window in Fig. 15 provide an inviting target for LHC wino pair production searches. In the case of $pp \rightarrow \tilde{\chi}_2^\pm \tilde{\chi}_3^0$ production, then the relevant signatures occur in the $VV + \cancel{E}_T$, $Vh + \cancel{E}_T$ and $hh + \cancel{E}_T$ channels, where $V = W$ or Z . While the strong ATLAS limits from boosted V or $H \rightarrow jj$ already exclude

$m_{3/2} : 200 - 350$ TeV, a search for non-boosted multijets+ \cancel{E}_T may be warranted for electroweak-produced wino pairs. These searches may be augmented by searching for the presence of $h \rightarrow b\bar{b}$ and $V \rightarrow leptons$ in the signal events. New targeted analyses using Run 2 data or forthcoming Run 3 data may even be able to close this allowed window (or else discover nAMSB SUSY!). Certainly the allowed window in nAMSB parameter space can be closed by analysis of HL-LHC data.

7.2.2 Same-sign diboson signature

The other lucrative search channel for wino pair production followed by decay to light higgsinos is the same-sign diboson channel (SSdB)[126], where $pp \rightarrow \tilde{\chi}_2^\pm \tilde{\chi}_3^0$ will be followed by $\tilde{\chi}_2^\pm \rightarrow W^\pm \tilde{\chi}_{1,2}^0$ and $\tilde{\chi}_3^0 \rightarrow W^\pm \tilde{\chi}_1^\mp$. These production and decay modes lead equally to $W^+W^- + \cancel{E}_T$ and $W^\pm W^\pm + \cancel{E}_T$ final states where the former has large SM backgrounds from WW and $t\bar{t}$ production whilst SM backgrounds for the latter SSdB signature are far smaller[126, 127, 128]. This relatively jet-free (only jets from initial state QCD radiation) signature is distinct from the usual same-sign dilepton signature arising from gluino and squark pair production which should be accompanied by many hard final state jets.

The reach of HL-LHC for the natural SUSY SSdB signature has been computed in Ref. [128] where peak signal cross sections after cuts reach the 0.03 fb level compared to total SM backgrounds of 0.005 fb. Whereas the present reach of LHC with 139 fb^{-1} is minimal at present (for the harder, high luminosity cuts advocated in Ref. [128]), the low wino mass $m(\text{wino}) \sim 300 - 600$ GeV region should be accessible to LHC Run 3 and HL-LHC data sets in the $300\text{-}3000 \text{ fb}^{-1}$ regime. Alternatively, a fresh analysis by the experimental groups using softer cuts for the low wino mass region is clearly warranted. So far, it seems no dedicated analysis of the SSdB signature from natural SUSY has been undertaken.

7.3 LHC stop pair production search: $pp \rightarrow \tilde{t}_1 \tilde{t}_1^*$

Another SUSY search channel for the nAMSB model is via light top squark pair production $pp \rightarrow \tilde{t}_1 \tilde{t}_1^*$ followed by $\tilde{t}_1 \rightarrow b\tilde{\chi}_1^+$ at $\sim 50\%$ and $\tilde{t}_1 \rightarrow t\tilde{\chi}_{1,2}^0$ each at $\sim 25\%$. The reach of HL-LHC for light top-squarks with these decay modes has been recently evaluated[97]. The 5σ discovery reach of HL-LHC with 3000 fb^{-1} was found to extend to $m_{\tilde{t}_1} \sim 1.7$ TeV while the 95% CL reach extended to $m_{\tilde{t}_1} \sim 2$ TeV. These sorts of search limits, performed within the NUHM2 model, are expected to pertain also to stop pair production within the nAMSB model.

8 Summary and conclusions

Supersymmetric models with anomaly-mediated SUSY breaking are well-motivated in several different SUSY breaking scenarios. In charged SUSY breaking (AMSB0), gauginos and A -terms have suppressed gravity-mediated masses but can gain dominant AMSB masses whilst scalar masses assume their usual gravity-mediated form. In the RS AMSB model with sequestered SUSY breaking, then gaugino masses, A -terms and scalar masses all have the AMSB form, leading to negative squared slepton masses. Further bulk scalar mass contributions are required for a viable model. The phenomenology of mAMSB models is characterized by a wino LSP, and

wino-like WIMP dark matter. The minimal phenomenological version of these models seems to be triply ruled out by 1. the difficulty to generate $m_h \sim 125$ GeV unless huge, unnatural third generation bulk scalar masses are included, 2. the presence of wino-like WIMP dark matter which seems excluded by direct- and indirect-dark matter detection limits and 3. the large, unnatural value of μ^- and hence large Δ_{EW^-} that such models possess, even for weak-scale soft terms. Rather minor tweaks to the mAMSB model, already suggested in the original work of RS[23], ameliorate these problems: non-universal bulk scalar Higgs masses and bulk A -terms. While AMSB0 with non-universal scalar masses still seems ruled out (due to $A_0 \sim 0$ and hence too low m_h values), the natural AMSB model is both natural and can accommodate $m_h \sim 125$ GeV. In nAMSB, while the wino is still the lightest gaugino, the higgsinos are instead the lightest EWinos. The dark matter issues can be resolved by postulating mixed axion-higgsino-like WIMP dark matter which is mainly coposed of axions[68].

In this work, we investigated in some detail LHC constraints on natural AMSB models. LHC gluino mass limits already require a gravitino mass $m_{3/2} \gtrsim 90$ TeV. The presence of relatively light winos with mass $m(\text{wino}) \sim 300 - 800$ GeV implies the model is susceptible to ATLAS/CMS searches for two boosted dijets + \cancel{E}_T . Recent ATLAS results seem to rule out $m_{3/2} \sim 200 - 350$ TeV, whereas naturalness ($\Delta_{EW} \lesssim 30$) requires $m_{3/2} \lesssim 265$ TeV. The combined constraints leave an open lower mass window of $m_{3/2} \sim 90 - 200$ TeV. This lower mass window may soon be excluded (or else nAMSB may be discovered!) by a combination of 1. soft OS dilepton plus jet+ \cancel{E}_T (OSDLJMET) searches which arise from higgsino pair production, 2. non-boosted hadronically decaying wino pair production searches and 3. jet-free same-sign diboson searches which are a characteristic signature of wino pair production followed by wino decay to $W + \text{higgsino}$. Some excess above SM background in the OSDLJMET channel already seems to be present in both ATLAS and CMS data[124, 119].

Acknowledgments

This material is based upon work supported by the U.S. Department of Energy, Office of Science, Office of High Energy Physics under Award Number DE-SC-0009956. VB gratefully acknowledges support from the William F. Vilas Estate.

References

- [1] D. J. H. Chung, L. L. Everett, G. L. Kane, S. F. King, J. D. Lykken, L.-T. Wang, The Soft supersymmetry breaking Lagrangian: Theory and applications, Phys. Rept. 407 (2005) 1–203. [arXiv:hep-ph/0312378](#), [doi:10.1016/j.physrep.2004.08.032](#).
- [2] G. F. Giudice, M. A. Luty, H. Murayama, R. Rattazzi, Gaugino mass without singlets, JHEP 12 (1998) 027. [arXiv:hep-ph/9810442](#), [doi:10.1088/1126-6708/1998/12/027](#).
- [3] E. Witten, Dynamical Breaking of Supersymmetry, Nucl. Phys. B 188 (1981) 513. [doi:10.1016/0550-3213\(81\)90006-7](#).

- [4] M. Dine, J. D. Mason, Supersymmetry and Its Dynamical Breaking, Rept. Prog. Phys. 74 (2011) 056201. [arXiv:1012.2836](#), [doi:10.1088/0034-4885/74/5/056201](#).
- [5] I. Affleck, M. Dine, N. Seiberg, Dynamical Supersymmetry Breaking in Four-Dimensions and Its Phenomenological Implications, Nucl. Phys. B 256 (1985) 557–599. [doi:10.1016/0550-3213\(85\)90408-0](#).
- [6] A. E. Nelson, A Viable model of dynamical supersymmetry breaking in the hidden sector, Phys. Lett. B 369 (1996) 277–282. [arXiv:hep-ph/9511350](#), [doi:10.1016/0370-2693\(95\)01547-7](#).
- [7] G. Lopes Cardoso, B. A. Ovrut, Supersymmetric calculation of mixed Kahler gauge and mixed Kahler-Lorentz anomalies, Nucl. Phys. B 418 (1994) 535–570. [arXiv:hep-th/9308066](#), [doi:10.1016/0550-3213\(94\)90530-4](#).
- [8] J. A. Bagger, T. Moroi, E. Poppitz, Anomaly mediation in supergravity theories, JHEP 04 (2000) 009. [arXiv:hep-th/9911029](#), [doi:10.1088/1126-6708/2000/04/009](#).
- [9] L. J. Dixon, V. Kaplunovsky, J. Louis, Moduli dependence of string loop corrections to gauge coupling constants, Nucl. Phys. B 355 (1991) 649–688. [doi:10.1016/0550-3213\(91\)90490-0](#).
- [10] M. Dine, D. MacIntire, Supersymmetry, naturalness, and dynamical supersymmetry breaking, Phys. Rev. D 46 (1992) 2594–2601. [arXiv:hep-ph/9205227](#), [doi:10.1103/PhysRevD.46.2594](#).
- [11] V. S. Kaplunovsky, J. Louis, Model independent analysis of soft terms in effective supergravity and in string theory, Phys. Lett. B 306 (1993) 269–275. [arXiv:hep-th/9303040](#), [doi:10.1016/0370-2693\(93\)90078-V](#).
- [12] V. Kaplunovsky, J. Louis, Field dependent gauge couplings in locally supersymmetric effective quantum field theories, Nucl. Phys. B 422 (1994) 57–124. [arXiv:hep-th/9402005](#), [doi:10.1016/0550-3213\(94\)00150-2](#).
- [13] J. D. Wells, Implications of supersymmetry breaking with a little hierarchy between gauginos and scalars, in: 11th International Conference on Supersymmetry and the Unification of Fundamental Interactions, 2003. [arXiv:hep-ph/0306127](#).
- [14] J. D. Wells, PeV-scale supersymmetry, Phys. Rev. D 71 (2005) 015013. [arXiv:hep-ph/0411041](#), [doi:10.1103/PhysRevD.71.015013](#).
- [15] N. Arkani-Hamed, S. Dimopoulos, Supersymmetric unification without low energy supersymmetry and signatures for fine-tuning at the LHC, JHEP 06 (2005) 073. [arXiv:hep-th/0405159](#), [doi:10.1088/1126-6708/2005/06/073](#).
- [16] N. Arkani-Hamed, S. Dimopoulos, G. F. Giudice, A. Romanino, Aspects of split supersymmetry, Nucl. Phys. B 709 (2005) 3–46. [arXiv:hep-ph/0409232](#), [doi:10.1016/j.nuclphysb.2004.12.026](#).

- [17] A. Arvanitaki, N. Craig, S. Dimopoulos, G. Villadoro, Mini-Split, *JHEP* 02 (2013) 126. [arXiv:1210.0555](#), [doi:10.1007/JHEP02\(2013\)126](#).
- [18] G. F. Giudice, A. Strumia, Probing High-Scale and Split Supersymmetry with Higgs Mass Measurements, *Nucl. Phys. B* 858 (2012) 63–83. [arXiv:1108.6077](#), [doi:10.1016/j.nuclphysb.2012.01.001](#).
- [19] M. Carena, H. E. Haber, Higgs Boson Theory and Phenomenology, *Prog. Part. Nucl. Phys.* 50 (2003) 63–152. [arXiv:hep-ph/0208209](#), [doi:10.1016/S0146-6410\(02\)00177-1](#).
- [20] H. Baer, V. Barger, A. Mustafayev, Implications of a 125 GeV Higgs scalar for LHC SUSY and neutralino dark matter searches, *Phys. Rev. D* 85 (2012) 075010. [arXiv:1112.3017](#), [doi:10.1103/PhysRevD.85.075010](#).
- [21] M. Dine, R. G. Leigh, A. Kagan, Flavor symmetries and the problem of squark degeneracy, *Phys. Rev. D* 48 (1993) 4269–4274. [arXiv:hep-ph/9304299](#), [doi:10.1103/PhysRevD.48.4269](#).
- [22] J. L. Feng, T. Moroi, L. Randall, M. Strassler, S.-f. Su, Discovering supersymmetry at the Tevatron in wino LSP scenarios, *Phys. Rev. Lett.* 83 (1999) 1731–1734. [arXiv:hep-ph/9904250](#), [doi:10.1103/PhysRevLett.83.1731](#).
- [23] L. Randall, R. Sundrum, Out of this world supersymmetry breaking, *Nucl. Phys. B* 557 (1999) 79–118. [arXiv:hep-th/9810155](#), [doi:10.1016/S0550-3213\(99\)00359-4](#).
- [24] M. Kawasaki, K. Kohri, T. Moroi, A. Yotsuyanagi, Big-Bang Nucleosynthesis and Gravitino, *Phys. Rev. D* 78 (2008) 065011. [arXiv:0804.3745](#), [doi:10.1103/PhysRevD.78.065011](#).
- [25] J. Pradler, F. D. Steffen, Thermal gravitino production and collider tests of leptogenesis, *Phys. Rev. D* 75 (2007) 023509. [arXiv:hep-ph/0608344](#), [doi:10.1103/PhysRevD.75.023509](#).
- [26] T. Moroi, L. Randall, Wino cold dark matter from anomaly mediated SUSY breaking, *Nucl. Phys. B* 570 (2000) 455–472. [arXiv:hep-ph/9906527](#), [doi:10.1016/S0550-3213\(99\)00748-8](#).
- [27] K. J. Bae, H. Baer, V. Barger, R. W. Deal, The cosmological moduli problem and naturalness, *JHEP* 02 (2022) 138. [arXiv:2201.06633](#), [doi:10.1007/JHEP02\(2022\)138](#).
- [28] M. K. Gaillard, B. D. Nelson, Quantum induced soft supersymmetry breaking in supergravity, *Nucl. Phys. B* 588 (2000) 197–212. [arXiv:hep-th/0004170](#), [doi:10.1016/S0550-3213\(00\)00494-6](#).
- [29] A. Anisimov, M. Dine, M. Graesser, S. D. Thomas, Brane world SUSY breaking, *Phys. Rev. D* 65 (2002) 105011. [arXiv:hep-th/0111235](#), [doi:10.1103/PhysRevD.65.105011](#).

- [30] A. Anisimov, M. Dine, M. Graesser, S. D. Thomas, Brane world SUSY breaking from string / M theory, JHEP 03 (2002) 036. [arXiv:hep-th/0201256](#), [doi:10.1088/1126-6708/2002/03/036](#).
- [31] M. A. Luty, 2004 TASI lectures on supersymmetry breaking, in: Theoretical Advanced Study Institute in Elementary Particle Physics: Physics in $D \geq 4$, 2005, pp. 495–582. [arXiv:hep-th/0509029](#).
- [32] D. R. T. Jones, G. G. Ross, Anomaly mediation and dimensional transmutation, Phys. Lett. B 642 (2006) 540–545. [arXiv:hep-ph/0609210](#), [doi:10.1016/j.physletb.2006.10.010](#).
- [33] M. Dine, N. Seiberg, Comments on quantum effects in supergravity theories, JHEP 03 (2007) 040. [arXiv:hep-th/0701023](#), [doi:10.1088/1126-6708/2007/03/040](#).
- [34] S. P. de Alwis, On Anomaly Mediated SUSY Breaking, Phys. Rev. D 77 (2008) 105020. [arXiv:0801.0578](#), [doi:10.1103/PhysRevD.77.105020](#).
- [35] H. Baer, S. de Alwis, K. Givens, S. Rajagopalan, H. Summy, Gaugino Anomaly Mediated SUSY Breaking: phenomenology and prospects for the LHC, JHEP 05 (2010) 069. [arXiv:1002.4633](#), [doi:10.1007/JHEP05\(2010\)069](#).
- [36] D.-W. Jung, J. Y. Lee, Anomaly-Mediated Supersymmetry Breaking Demystified, JHEP 03 (2009) 123. [arXiv:0902.0464](#), [doi:10.1088/1126-6708/2009/03/123](#).
- [37] D. Sanford, Y. Shirman, Anomaly Mediation from Randall-Sundrum to Dine-Seiberg, Phys. Rev. D 83 (2011) 125020. [arXiv:1012.1860](#), [doi:10.1103/PhysRevD.83.125020](#).
- [38] J. P. Conlon, M. Goodsell, E. Palti, Anomaly Mediation in Superstring Theory, Fortsch. Phys. 59 (2011) 5–75. [arXiv:1008.4361](#), [doi:10.1002/prop.201000087](#).
- [39] F. D’Eramo, J. Thaler, Z. Thomas, The Two Faces of Anomaly Mediation, JHEP 06 (2012) 151. [arXiv:1202.1280](#), [doi:10.1007/JHEP06\(2012\)151](#).
- [40] F. D’Eramo, J. Thaler, Z. Thomas, Anomaly Mediation from Unbroken Supergravity, JHEP 09 (2013) 125. [arXiv:1307.3251](#), [doi:10.1007/JHEP09\(2013\)125](#).
- [41] M. Dine, P. Draper, Anomaly Mediation in Local Effective Theories, JHEP 02 (2014) 069. [arXiv:1310.2196](#), [doi:10.1007/JHEP02\(2014\)069](#).
- [42] S. P. de Alwis, AMSB and the Logic of Spontaneous SUSY Breaking, JHEP 01 (2013) 006. [arXiv:1206.6775](#), [doi:10.1007/JHEP01\(2013\)006](#).
- [43] K. Harigaya, M. Ibe, Anomaly Mediated Gaugino Mass and Path-Integral Measure, Phys. Rev. D 90 (8) (2014) 085028. [arXiv:1409.5029](#), [doi:10.1103/PhysRevD.90.085028](#).
- [44] M. Luty, R. Sundrum, Anomaly mediated supersymmetry breaking in four-dimensions, naturally, Phys. Rev. D 67 (2003) 045007. [arXiv:hep-th/0111231](#), [doi:10.1103/PhysRevD.67.045007](#).

- [45] M. Dine, P. J. Fox, E. Gorbatov, Y. Shadmi, Y. Shirman, S. D. Thomas, Visible effects of the hidden sector, *Phys. Rev. D* 70 (2004) 045023. [arXiv:hep-ph/0405159](#), doi:10.1103/PhysRevD.70.045023.
- [46] M. Ibe, K. I. Izawa, Y. Nakayama, Y. Shinbara, T. Yanagida, Conformally sequestered SUSY breaking in vector-like gauge theories, *Phys. Rev. D* 73 (2006) 015004. [arXiv:hep-ph/0506023](#), doi:10.1103/PhysRevD.73.015004.
- [47] H. Murayama, Y. Nomura, D. Poland, More visible effects of the hidden sector, *Phys. Rev. D* 77 (2008) 015005. [arXiv:0709.0775](#), doi:10.1103/PhysRevD.77.015005.
- [48] T. Gherghetta, G. F. Giudice, J. D. Wells, Phenomenological consequences of supersymmetry with anomaly induced masses, *Nucl. Phys. B* 559 (1999) 27–47. [arXiv:hep-ph/9904378](#), doi:10.1016/S0550-3213(99)00429-0.
- [49] J. L. Feng, T. Moroi, Supernatural supersymmetry: Phenomenological implications of anomaly mediated supersymmetry breaking, *Phys. Rev. D* 61 (2000) 095004. [arXiv:hep-ph/9907319](#), doi:10.1103/PhysRevD.61.095004.
- [50] F. E. Paige, J. D. Wells, Anomaly mediated SUSY breaking at the LHC, in: 1st Les Houches Workshop on Physics at TeV Colliders, 1999. [arXiv:hep-ph/0001249](#).
- [51] H. Baer, J. K. Mizukoshi, X. Tata, Reach of the CERN LHC for the minimal anomaly mediated SUSY breaking model, *Phys. Lett. B* 488 (2000) 367–372. [arXiv:hep-ph/0007073](#), doi:10.1016/S0370-2693(00)00925-4.
- [52] A. J. Barr, C. G. Lester, M. A. Parker, B. C. Allanach, P. Richardson, Discovering anomaly mediated supersymmetry at the LHC, *JHEP* 03 (2003) 045. [arXiv:hep-ph/0208214](#), doi:10.1088/1126-6708/2003/03/045.
- [53] B. C. Allanach, T. J. Khoo, K. Sakurai, Interpreting a 1 fb^{-1} ATLAS Search in the Minimal Anomaly Mediated Supersymmetry Breaking Model, *JHEP* 11 (2011) 132. [arXiv:1110.1119](#), doi:10.1007/JHEP11(2011)132.
- [54] E. Bagnaschi, et al., Likelihood Analysis of the Minimal AMSB Model, *Eur. Phys. J. C* 77 (4) (2017) 268. [arXiv:1612.05210](#), doi:10.1140/epjc/s10052-017-4810-0.
- [55] H. Baer, V. Barger, D. Mickelson, M. Padeffke-Kirkland, SUSY models under siege: LHC constraints and electroweak fine-tuning, *Phys. Rev. D* 89 (11) (2014) 115019. [arXiv:1404.2277](#), doi:10.1103/PhysRevD.89.115019.
- [56] H. Baer, V. Barger, P. Huang, A. Mustafayev, X. Tata, Radiative natural SUSY with a 125 GeV Higgs boson, *Phys. Rev. Lett.* 109 (2012) 161802. [arXiv:1207.3343](#), doi:10.1103/PhysRevLett.109.161802.
- [57] H. Baer, V. Barger, P. Huang, D. Mickelson, A. Mustafayev, X. Tata, Radiative natural supersymmetry: Reconciling electroweak fine-tuning and the Higgs boson mass, *Phys. Rev. D* 87 (11) (2013) 115028. [arXiv:1212.2655](#), doi:10.1103/PhysRevD.87.115028.

- [58] A. Arbey, M. Battaglia, A. Djouadi, F. Mahmoudi, J. Quevillon, Implications of a 125 GeV Higgs for supersymmetric models, *Phys. Lett. B* 708 (2012) 162–169. [arXiv:1112.3028](#), [doi:10.1016/j.physletb.2012.01.053](#).
- [59] H. Baer, V. Barger, A. Mustafayev, Neutralino dark matter in mSUGRA/CMSSM with a 125 GeV light Higgs scalar, *JHEP* 05 (2012) 091. [arXiv:1202.4038](#), [doi:10.1007/JHEP05\(2012\)091](#).
- [60] T. Cohen, M. Lisanti, A. Pierce, T. R. Slatyer, Wino Dark Matter Under Siege, *JCAP* 10 (2013) 061. [arXiv:1307.4082](#), [doi:10.1088/1475-7516/2013/10/061](#).
- [61] J. Fan, M. Reece, In Wino Veritas? Indirect Searches Shed Light on Neutralino Dark Matter, *JHEP* 10 (2013) 124. [arXiv:1307.4400](#), [doi:10.1007/JHEP10\(2013\)124](#).
- [62] H. Baer, V. Barger, H. Serce, SUSY under siege from direct and indirect WIMP detection experiments, *Phys. Rev. D* 94 (11) (2016) 115019. [arXiv:1609.06735](#), [doi:10.1103/PhysRevD.94.115019](#).
- [63] K. J. Bae, H. Baer, A. Lessa, H. Serce, Mixed axion-wino dark matter, *Front. in Phys.* 3 (2015) 49. [arXiv:1502.07198](#), [doi:10.3389/fphy.2015.00049](#).
- [64] H. Baer, V. Barger, D. Sengupta, Anomaly mediated SUSY breaking model retrofitted for naturalness, *Phys. Rev. D* 98 (1) (2018) 015039. [arXiv:1801.09730](#), [doi:10.1103/PhysRevD.98.015039](#).
- [65] P. Slavich, et al., Higgs-mass predictions in the MSSM and beyond, *Eur. Phys. J. C* 81 (5) (2021) 450. [arXiv:2012.15629](#), [doi:10.1140/epjc/s10052-021-09198-2](#).
- [66] J. R. Ellis, K. A. Olive, Y. Santoso, The MSSM parameter space with nonuniversal Higgs masses, *Phys. Lett. B* 539 (2002) 107–118. [arXiv:hep-ph/0204192](#), [doi:10.1016/S0370-2693\(02\)02071-3](#).
- [67] H. Baer, A. Mustafayev, S. Profumo, A. Belyaev, X. Tata, Direct, indirect and collider detection of neutralino dark matter in SUSY models with non-universal Higgs masses, *JHEP* 07 (2005) 065. [arXiv:hep-ph/0504001](#), [doi:10.1088/1126-6708/2005/07/065](#).
- [68] H. Baer, A. Lessa, S. Rajagopalan, W. Sreethawong, Mixed axion/neutralino cold dark matter in supersymmetric models, *JCAP* 06 (2011) 031. [arXiv:1103.5413](#), [doi:10.1088/1475-7516/2011/06/031](#).
- [69] K. J. Bae, H. Baer, E. J. Chun, Mixed axion/neutralino dark matter in the SUSY DFSZ axion model, *JCAP* 12 (2013) 028. [arXiv:1309.5365](#), [doi:10.1088/1475-7516/2013/12/028](#).
- [70] R. Bousso, J. Polchinski, Quantization of four form fluxes and dynamical neutralization of the cosmological constant, *JHEP* 06 (2000) 006. [arXiv:hep-th/0004134](#), [doi:10.1088/1126-6708/2000/06/006](#).

- [71] L. Susskind, The Anthropic landscape of string theory (2003) 247–266 [arXiv:hep-th/0302219](#).
- [72] M. R. Douglas, S. Kachru, Flux compactification, *Rev. Mod. Phys.* 79 (2007) 733–796. [arXiv:hep-th/0610102](#), [doi:10.1103/RevModPhys.79.733](#).
- [73] M. R. Douglas, The Statistics of string / M theory vacua, *JHEP* 05 (2003) 046. [arXiv:hep-th/0303194](#), [doi:10.1088/1126-6708/2003/05/046](#).
- [74] S. Ashok, M. R. Douglas, Counting flux vacua, *JHEP* 01 (2004) 060. [arXiv:hep-th/0307049](#), [doi:10.1088/1126-6708/2004/01/060](#).
- [75] W. Taylor, Y.-N. Wang, The F-theory geometry with most flux vacua, *JHEP* 12 (2015) 164. [arXiv:1511.03209](#), [doi:10.1007/JHEP12\(2015\)164](#).
- [76] S. Weinberg, Anthropic Bound on the Cosmological Constant, *Phys. Rev. Lett.* 59 (1987) 2607. [doi:10.1103/PhysRevLett.59.2607](#).
- [77] G. F. Giudice, A. Romanino, Split supersymmetry, *Nucl. Phys. B* 699 (2004) 65–89, [Erratum: *Nucl.Phys.B* 706, 487–487 (2005)]. [arXiv:hep-ph/0406088](#), [doi:10.1016/j.nuclphysb.2004.08.001](#).
- [78] E. Bagnaschi, G. F. Giudice, P. Slavich, A. Strumia, Higgs Mass and Unnatural Supersymmetry, *JHEP* 09 (2014) 092. [arXiv:1407.4081](#), [doi:10.1007/JHEP09\(2014\)092](#).
- [79] N. Arkani-Hamed, A. Gupta, D. E. Kaplan, N. Weiner, T. Zorawski, Simply Unnatural Supersymmetry (12 2012). [arXiv:1212.6971](#).
- [80] H. Baer, V. Barger, D. Martinez, S. Salam, Radiative natural supersymmetry emergent from the string landscape, *JHEP* 03 (2022) 186. [arXiv:2202.07046](#), [doi:10.1007/JHEP03\(2022\)186](#).
- [81] V. Agrawal, S. M. Barr, J. F. Donoghue, D. Seckel, Viable range of the mass scale of the standard model, *Phys. Rev. D* 57 (1998) 5480–5492. [arXiv:hep-ph/9707380](#), [doi:10.1103/PhysRevD.57.5480](#).
- [82] H. Baer, V. Barger, D. Martinez, S. Salam, Fine-tuned vs. natural supersymmetry: what does the string landscape predict?, *JHEP* 09 (2022) 125. [arXiv:2206.14839](#), [doi:10.1007/JHEP09\(2022\)125](#).
- [83] G. L. Kane, C. F. Kolda, L. Roszkowski, J. D. Wells, Study of constrained minimal supersymmetry, *Phys. Rev. D* 49 (1994) 6173–6210. [arXiv:hep-ph/9312272](#), [doi:10.1103/PhysRevD.49.6173](#).
- [84] L. J. Hall, Y. Nomura, Spread Supersymmetry, *JHEP* 01 (2012) 082. [arXiv:1111.4519](#), [doi:10.1007/JHEP01\(2012\)082](#).

- [85] V. Barger, J. Jiang, P. Langacker, T. Li, Non-canonical gauge coupling unification in high-scale supersymmetry breaking, *Nucl. Phys. B* 726 (2005) 149–170. [arXiv:hep-ph/0504093](#), [doi:10.1016/j.nuclphysb.2005.08.007](#).
- [86] B. S. Acharya, K. Bobkov, G. L. Kane, J. Shao, P. Kumar, The G(2)-MSSM: An M Theory motivated model of Particle Physics, *Phys. Rev. D* 78 (2008) 065038. [arXiv:0801.0478](#), [doi:10.1103/PhysRevD.78.065038](#).
- [87] M. R. Douglas, Statistical analysis of the supersymmetry breaking scale (5, 2004). [arXiv:hep-th/0405279](#).
- [88] H. P. Nilles, P. K. S. Vaudrevange, Geography of Fields in Extra Dimensions: String Theory Lessons for Particle Physics, *Mod. Phys. Lett. A* 30 (10) (2015) 1530008. [arXiv:1403.1597](#), [doi:10.1142/S0217732315300086](#).
- [89] H. Baer, V. Barger, S. Salam, D. Sengupta, String landscape guide to soft SUSY breaking terms, *Phys. Rev. D* 102 (7) (2020) 075012. [arXiv:2005.13577](#), [doi:10.1103/PhysRevD.102.075012](#).
- [90] H. Baer, V. Barger, H. Serce, K. Sinha, Higgs and superparticle mass predictions from the landscape, *JHEP* 03 (2018) 002. [arXiv:1712.01399](#), [doi:10.1007/JHEP03\(2018\)002](#).
- [91] H. Baer, V. Barger, D. Sengupta, Mirage mediation from the landscape, *Phys. Rev. Res.* 2 (1) (2020) 013346. [arXiv:1912.01672](#), [doi:10.1103/PhysRevResearch.2.013346](#).
- [92] H. Baer, V. Barger, X. Tata, K. Zhang, Prospects for Heavy Neutral SUSY HIGGS Scalars in the hMSSM and Natural SUSY at LHC Upgrades, *Symmetry* 14 (10) (2022) 2061. [arXiv:2209.00063](#), [doi:10.3390/sym14102061](#).
- [93] H. Baer, V. Barger, D. Sengupta, Landscape solution to the SUSY flavor and CP problems, *Phys. Rev. Res.* 1 (3) (2019) 033179. [arXiv:1910.00090](#), [doi:10.1103/PhysRevResearch.1.033179](#).
- [94] H. Baer, V. Barger, M. Savoy, H. Serce, The Higgs mass and natural supersymmetric spectrum from the landscape, *Phys. Lett. B* 758 (2016) 113–117. [arXiv:1602.07697](#), [doi:10.1016/j.physletb.2016.05.010](#).
- [95] H. Baer, V. Barger, S. Salam, Naturalness versus stringy naturalness (with implications for collider and dark matter searches, *Phys. Rev. Research.* 1 (2019) 023001. [arXiv:1906.07741](#), [doi:10.1103/PhysRevResearch.1.023001](#).
- [96] H. Baer, V. Barger, J. S. Gainer, P. Huang, M. Savoy, D. Sengupta, X. Tata, Gluino reach and mass extraction at the LHC in radiatively-driven natural SUSY, *Eur. Phys. J. C* 77 (7) (2017) 499. [arXiv:1612.00795](#), [doi:10.1140/epjc/s10052-017-5067-3](#).
- [97] H. Baer, V. Barger, J. Dutta, D. Sengupta, K. Zhang, Top squarks from the landscape at high luminosity LHC (7 2023). [arXiv:2307.08067](#).

- [98] F. E. Paige, S. D. Protopopescu, H. Baer, X. Tata, ISAJET 7.69: A Monte Carlo event generator for pp, anti-p p, and e+e- reactions (12 2003). [arXiv:hep-ph/0312045](#).
- [99] W. Beenakker, R. Hopker, M. Spira, PROSPINO: A Program for the production of supersymmetric particles in next-to-leading order QCD (11 1996). [arXiv:hep-ph/9611232](#).
- [100] P. Z. Skands, et al., SUSY Les Houches accord: Interfacing SUSY spectrum calculators, decay packages, and event generators, JHEP 07 (2004) 036. [arXiv:hep-ph/0311123](#), [doi:10.1088/1126-6708/2004/07/036](#).
- [101] H. Baer, X. Tata, Weak scale supersymmetry: From superfields to scattering events, Cambridge University Press, 2006.
- [102] Z. Han, G. D. Kribs, A. Martin, A. Menon, Hunting quasidegenerate Higgsinos, Phys. Rev. D 89 (7) (2014) 075007. [arXiv:1401.1235](#), [doi:10.1103/PhysRevD.89.075007](#).
- [103] H. Baer, A. Mustafayev, X. Tata, Monojet plus soft dilepton signal from light higgsino pair production at LHC14, Phys. Rev. D 90 (11) (2014) 115007. [arXiv:1409.7058](#), [doi:10.1103/PhysRevD.90.115007](#).
- [104] K. J. Bae, H. Baer, V. Barger, D. Sengupta, Revisiting the SUSY μ problem and its solutions in the LHC era, Phys. Rev. D 99 (11) (2019) 115027. [arXiv:1902.10748](#), [doi:10.1103/PhysRevD.99.115027](#).
- [105] H. Baer, V. Barger, N. Nagata, M. Savoy, Phenomenological profile of top squarks from natural supersymmetry at the LHC, Phys. Rev. D 95 (5) (2017) 055012, [Addendum: Phys.Rev.D 103, 059902 (2021)]. [arXiv:1611.08511](#), [doi:10.1103/PhysRevD.95.055012](#).
- [106] G. Aad, et al., Search for supersymmetry in final states with missing transverse momentum and three or more b-jets in 139 fb^{-1} of proton-proton collisions at $\sqrt{s} = 13 \text{ TeV}$ with the ATLAS detector, Eur. Phys. J. C 83 (7) (2023) 561. [arXiv:2211.08028](#), [doi:10.1140/epjc/s10052-023-11543-6](#).
- [107] T. C. Collaboration, et al., Search for supersymmetry in proton-proton collisions at 13 TeV in final states with jets and missing transverse momentum, JHEP 10 (2019) 244. [arXiv:1908.04722](#), [doi:10.1007/JHEP10\(2019\)244](#).
- [108] A. M. Sirunyan, et al., Searches for physics beyond the standard model with the M_{T2} variable in hadronic final states with and without disappearing tracks in proton-proton collisions at $\sqrt{s} = 13 \text{ TeV}$, Eur. Phys. J. C 80 (1) (2020) 3. [arXiv:1909.03460](#), [doi:10.1140/epjc/s10052-019-7493-x](#).
- [109] G. Aad, et al., Search for charginos and neutralinos in final states with two boosted hadronically decaying bosons and missing transverse momentum in pp collisions at $\sqrt{s} = 13 \text{ TeV}$ with the ATLAS detector, Phys. Rev. D 104 (11) (2021) 112010. [arXiv:2108.07586](#), [doi:10.1103/PhysRevD.104.112010](#).

- [110] A. Tumasyan, et al., Search for electroweak production of charginos and neutralinos at $s=13\text{TeV}$ in final states containing hadronic decays of WW, WZ, or WH and missing transverse momentum, Phys. Lett. B 842 (2023) 137460. [arXiv:2205.09597](#), [doi:10.1016/j.physletb.2022.137460](#).
- [111] S. Kraml, S. Kulkarni, U. Laa, A. Lessa, W. Magerl, D. Proschofsky-Spindler, W. Waltenberger, SModelS: a tool for interpreting simplified-model results from the LHC and its application to supersymmetry, Eur. Phys. J. C 74 (2014) 2868. [arXiv:1312.4175](#), [doi:10.1140/epjc/s10052-014-2868-5](#).
- [112] F. Ambrogio, et al., SModelS v1.2: long-lived particles, combination of signal regions, and other novelties, Comput. Phys. Commun. 251 (2020) 106848. [arXiv:1811.10624](#), [doi:10.1016/j.cpc.2019.07.013](#).
- [113] G. Alguero, J. Heisig, C. K. Khosa, S. Kraml, S. Kulkarni, A. Lessa, H. Reyes-González, W. Waltenberger, A. Wongel, Constraining new physics with SModelS version 2, JHEP 08 (2022) 068. [arXiv:2112.00769](#), [doi:10.1007/JHEP08\(2022\)068](#).
- [114] M. Drees, H. Dreiner, D. Schmeier, J. Tattersall, J. S. Kim, CheckMATE: Confronting your Favourite New Physics Model with LHC Data, Comput. Phys. Commun. 187 (2015) 227–265. [arXiv:1312.2591](#), [doi:10.1016/j.cpc.2014.10.018](#).
- [115] D. Dercks, N. Desai, J. S. Kim, K. Rolbiecki, J. Tattersall, T. Weber, CheckMATE 2: From the model to the limit, Comput. Phys. Commun. 221 (2017) 383–418. [arXiv:1611.09856](#), [doi:10.1016/j.cpc.2017.08.021](#).
- [116] A. M. Sirunyan, et al., Search for electroweak production of charginos and neutralinos in multilepton final states in proton-proton collisions at $\sqrt{s} = 13\text{ TeV}$, JHEP 03 (2018) 166. [arXiv:1709.05406](#), [doi:10.1007/JHEP03\(2018\)166](#).
- [117] Search for squarks and gluinos in final states with jets and missing transverse momentum using 139 fb^{-1} of $\sqrt{s} = 13\text{ TeV}$ pp collision data with the ATLAS detector (8 2019).
- [118] G. Aad, et al., Search for chargino–neutralino pair production in final states with three leptons and missing transverse momentum in $\sqrt{s} = 13\text{ TeV}$ pp collisions with the ATLAS detector, Eur. Phys. J. C 81 (12) (2021) 1118. [arXiv:2106.01676](#), [doi:10.1140/epjc/s10052-021-09749-7](#).
- [119] A. Tumasyan, et al., Search for supersymmetry in final states with two or three soft leptons and missing transverse momentum in proton-proton collisions at $\sqrt{s} = 13\text{ TeV}$, JHEP 04 (2022) 091. [arXiv:2111.06296](#), [doi:10.1007/JHEP04\(2022\)091](#).
- [120] M. Aaboud, et al., Search for squarks and gluinos in final states with jets and missing transverse momentum using 36 fb^{-1} of $\sqrt{s} = 13\text{ TeV}$ pp collision data with the ATLAS detector, Phys. Rev. D 97 (11) (2018) 112001. [arXiv:1712.02332](#), [doi:10.1103/PhysRevD.97.112001](#).

- [121] H. Baer, V. Barger, P. Huang, Hidden SUSY at the LHC: the light higgsino-world scenario and the role of a lepton collider, *JHEP* 11 (2011) 031. [arXiv:1107.5581](#), [doi:10.1007/JHEP11\(2011\)031](#).
- [122] H. Baer, V. Barger, S. Salam, D. Sengupta, X. Tata, The LHC higgsino discovery plane for present and future SUSY searches, *Phys. Lett. B* 810 (2020) 135777. [arXiv:2007.09252](#), [doi:10.1016/j.physletb.2020.135777](#).
- [123] H. Baer, V. Barger, D. Sengupta, X. Tata, New angular and other cuts to improve the Higgsino signal at the LHC, *Phys. Rev. D* 105 (9) (2022) 095017. [arXiv:2109.14030](#), [doi:10.1103/PhysRevD.105.095017](#).
- [124] G. Aad, et al., Searches for electroweak production of supersymmetric particles with compressed mass spectra in $\sqrt{s} = 13$ TeV pp collisions with the ATLAS detector, *Phys. Rev. D* 101 (5) (2020) 052005. [arXiv:1911.12606](#), [doi:10.1103/PhysRevD.101.052005](#).
- [125] A. Canepa, T. Han, X. Wang, The Search for Electroweakinos, *Ann. Rev. Nucl. Part. Sci.* 70 (2020) 425–454. [arXiv:2003.05450](#), [doi:10.1146/annurev-nucl-031020-121031](#).
- [126] H. Baer, V. Barger, P. Huang, D. Mickelson, A. Mustafayev, W. Sreethawong, X. Tata, Same sign diboson signature from supersymmetry models with light higgsinos at the LHC, *Phys. Rev. Lett.* 110 (15) (2013) 151801. [arXiv:1302.5816](#), [doi:10.1103/PhysRevLett.110.151801](#).
- [127] H. Baer, V. Barger, P. Huang, D. Mickelson, A. Mustafayev, W. Sreethawong, X. Tata, Radiatively-driven natural supersymmetry at the LHC, *JHEP* 12 (2013) 013, [Erratum: *JHEP* 06, 053 (2015)]. [arXiv:1310.4858](#), [doi:10.1007/JHEP12\(2013\)013](#).
- [128] H. Baer, V. Barger, J. S. Gainer, M. Savoy, D. Sengupta, X. Tata, Aspects of the same-sign diboson signature from wino pair production with light higgsinos at the high luminosity LHC, *Phys. Rev. D* 97 (3) (2018) 035012. [arXiv:1710.09103](#), [doi:10.1103/PhysRevD.97.035012](#).